Designing dynamic water storage systems to mitigate drought stress in urban environments

Investigating methods to design a digital representation of the Bajeskwartier water system

Amsterdam

September 2023

MSc Metropolitan Analysis, Design and Engineering
Master Thesis

Author:
Luka de Koe

Supervisors:
Alessio Belmondo Bianchi Di Lavagna MSc
Department of Agrotechnology and Food Sciences
Wageningen University & Research

dr. Jess Wreyford

Department of Environmental Sciences
Wageningen University & Research

Abstract

As a result of ongoing climate change, urban environments are put under increasing pressure from extreme weather events. Insufficient research is being done into the modeling of urban drought resilience. Most urban drought resilience and water network optimization models are designed for city-scale demand with regional water supply networks and vegetation water demand models generally address agricultural systems. This research addresses this gap by developing a neighborhood-scale digital representation of the Bajeskwartier water system to assess drought resilience while incorporating the local vegetation water demand. Starting with a system thinking perspective, the interconnections of soil moisture processes in the local water systems provide the base of the model.

By incorporating scenario analyses on climate change projections and vegetation types, the water demand and drought sensitivity patterns become clear. Furthermore, the implementation of an optimization solver to assess a rainwater capture, storage, and irrigation system results in a robust water system. The system proves to have sufficient capacity to prevent drought stress in a 1-in-30-year drought.

This research not only contributes to enhancing urban drought resilience within the Bajeskwartier but also provides a valuable foundation for future studies in similar urban contexts. It emphasizes the importance of considering local vegetation water demand and climate change scenarios in urban water system modeling, highlighting the need for tailored approaches to address evolving climate-induced challenges in urban environments.

List of symbols and acronyms

Cp: Specific heat of moist air
DP: Deep percolation
Dw: Groundwater depth
Dwc: Critical groundwater depth
ea: actual vapor pressure
ET0: Reference evapotranspiration
ETa: Actual evapotranspiration
FAO: Food and Agricultural Organization of the United Nations
GC: Groundwater contribution
Gmax: Steady upward flux
I: Irrigation
Kc: Crop coefficient
Ks: Water stress coefficient
MC: Moisture content
MIP: Mixed-Integer Programming
N: Total hours of sunlight
P: Precipitation
Qrt: Flow from the roof to the storage
Qti: Flow from the storage to the irrigation system
Rns: Net incoming solar radiation
Rnl: Net outgoing longwave radiation
RO: Runoff
rs: Fixed surface resistance
S_cap: Maximum storage capacity needed for each zone
T: Time
V: Volume in the water storage tank
W: Actual soil water storage
Wc: Critical water storage
Ws: Steady soil water storage
Y: The maximum potential daily rainwater yield
zr: Rooting depth
Z: Zones
α: Albedo
λ: Latent heat of vaporization
σ: Stefan-Boltzmann constant
θ: Soil moisture content
θfc: Field capacity moisture content
θwp: Wilting point moisture content
θa: Threshold moisture content
θs: Soil saturation moisture content
ρα: Air density
γ: Psychometric constant

Contents

1. Introduction

Urban environments are increasingly put under the pressure of extreme weather conditions (Balogun et al., 2020). The Intergovernmental Panel on Climate Change (IPCC) states that anthropogenic forcing has changed weather patterns, increasing the intensity and frequency of extreme weather events (Seneviratne et al., 2021). As seen in the summers of 2021 and 2022, long periods of drought and extreme rainfall events are becoming more common in the Netherlands (KNMI, 2021, 2022). In the summer of 2021, heavy rainfall resulted in severe flooding in the southern part of the province of Limburg. The summer of 2022 has been twice as dry as usual in the Netherlands and can be seen as an example of the droughts that are expected for the future (KNMI, 2022). As the effects of climate change are already noticeable, it is important to adapt urban environments to become more resilient to extreme weather. Alongside climate change mitigation measures, climate adaptation is an important part of ensuring the well-being of urban dwellers in the shorter term (Foster et al., 2011). Climate adaptation includes modifications to the urban fabric that can decrease heat stress, prevent flooding, and sewage overflow, among others.

The redevelopment of the Bajeskwartier in Amsterdam East presents ambitious plans to build a neighborhood of the future. With many innovations considered, the Bajes Kwartier Ontwikkeling planning company has put a large emphasis on climate adaptation through the use of blue-green infrastructure (AM & Fabrications, 2020). The blue-green infrastructure has been designed to benefit heat stress mitigation, slow down peak runoff, create buffer capacity with water storage, and benefit the well-being of the residents by creating a healthy and green environment. The plans show that most emphasis has been put on water drainage to mitigate flooding or sewage problems during extreme rainfall events, as well as the way greenspaces can ensure heat stress reduction (AM & Fabrications, 2020). However, little attention has been given to the resilience of the blue-green infrastructure in times of persisting drought. The frequency and intensity of extreme heat have increased since 1950 and will continue to rise (Seneviratne et al., 2021). Droughts in the form of rainfall deficit follow the same trend (Seneviratne et al., 2021). When periods of prolonged drought occur, the municipality of Amsterdam does not allow the use of tap water or nearby surface water for irrigation of green space. With increasing intensity and frequency of drought in the future, it can occur that the vegetation will suffer from severe drought stress. Therefore, a deeper understanding must be gained of the local water system and blue-green infrastructure regarding future water requirements.

In the context of urban water systems, digitization can improve the effectiveness of climate adaptation measures (Balogun et al., 2020). Preliminary and real-time data analyses can reveal patterns and behavior of complex systems, which might not be apparent at first glance (Arnold & Wade, 2015). As climate change is a process that will continue into the foreseeable future, it is important to assess the resilience of urban areas with potential future climate states in mind (Lawrence et al., 2021). Climate change scenarios can help understand the way climate change will unfold and how different emission rates influence the rate at which the climate changes. When used well, climate scenarios can support governance institutes to plan climate-proof urban development (Star et al., 2016).

1.1 Problem statement

In the field of urban water system modeling, most urban drought resilience and water network optimization models are designed for city-scale demand with regional water supply networks (Fooladivanda & Taylor, 2015; D'Ambrosio et al., 2015). Additionally, most research aims to account for public and non-public water demand in urban areas and little attention is paid to green infrastructure (Murgatroyd et al., 2022; D'Ambrosio et al., 2015). This results in a lack

of water demand calculation methods for urban green infrastructure. As the Bajeskwartier drought resilience assessment requires data on local water demand for the green infrastructure, an adaptation must be made to these existing models. The most common way to assess the water demand for vegetation is to calculate the evapotranspiration (Duarte Rocha et al., 2022). This method is mostly used in agricultural crop yield management tools (Castellaro et al., 2010). Applications of the commonly used Penman-Monteith-based evapotranspiration models predominantly assess the water demand of (mostly) homogenous vegetation in agriculture (Duarte Rocha et al., 2022). For a complex urban environment with different plant species spread across fragmented green spaces, a more elaborate evapotranspiration modeling approach is required. A new modeling method integrating an evapotranspiration model and water resource allocation optimization will be designed for the Bajeskwartier case. While designing the model, adaptability will be taken into account to ensure replicability and adoption in other contexts and projects.

1.2 Research Aim

This research aims to create a digital representation of the Bajeskwartier water system to assess drought resilience. The water balance and evapotranspiration characteristics of the green infrastructure will be investigated based on climate change scenarios. This preliminary assessment can be used to design adaptations to the current Bajeskwartier plans to implement an on-site rainwater capture, storage, and irrigation system. This way, the health of the greenspace can be ensured even in the most extreme drought cases.

The research question for this thesis is: *What modeling approaches can assess the Bajeskwartier drought resilience under a future climate change scenario?*

To answer the research question, the following sub-research questions are used:

SRQ1: *What is the water balance and what are the primary boundaries of the Bajeskwartier water system?*
SRQ2: *What climate change forecasting tool can be used to model extreme drought scenarios?*
SRQ3: *In what way does the system respond to different evapotranspiration rates of vegetation types?*
SRQ4: *In what way can on-site water storage facilities be coordinated to provide enough water for irrigation?*
SRQ5: *What interventions can improve the drought resilience of the Bajeskwartier?*

1.3 Scope of the research

This upfront assessment of the drought resilience of green infrastructure will be done for the Bajeskwartier developers, to support their design process of futureproof greenspace. Besides, the methodology in this research will be designed as such so it can be adapted and used in other projects in different urban environments, as climate change induced droughts is a worldwide issue. The proposed drought resilience assessment will be adaptable to other cases to enhance the design of urban greenspace.

2. Theoretical framework

In the process assessment of the Bajeskwartier water system, this thesis incorporates a structured three-part theoretical framework. This framework provides a systematic approach that incorporates systems thinking, scenario planning, and optimal water resource allocation theories. Through the framework integration, a step-wise approach is created to form the foundation onto which the research methods are built. The initial step of understanding the water system will be taken by using the systems thinking approach. By dissecting the system behavior, a digital representation can be made where the scenario planning approach can be implemented to see how the water system is affected by various climatological and biological conditions. This planning approach ties into the optimal water resource allocation theory where an optimization problem can be tested according to multiple scenarios.

While this theoretical framework presents a linear stepwise approach at first sight, the three steps will benefit the others in an iterative approach. The connection between the steps is shown in Figure 2.1. When assessing the scenario planning, for example, new insights into the complex system of the Bajeskwartier might arise. Therefore, each step will include a critical reflection of the knowledge gained in the other steps. The following sections of Chapter 2 will elaborate on each aspect of the framework, highlighting the theories that form the foundation of this research. Systems thinking will be explored in section 2.1, scenario planning in section 2.2, and optimal water resource allocation in section 2.3. In section 2.4, the way the theories are integrated into the methods will be outlined.

Figure 2.1: schematic overview of the theoretical framework

2.1 Systems thinking

Complex systems are becoming increasingly known throughout the world. They are found in the natural environment as well as human-constructed systems such as international trade and power networks (Arnold & Wade, 2015). These systems have deep connections and feedback loops which are difficult to predict. System thinking is a way of understanding the deep connections and underlying feedback loops (Arnold & Wade, 2015). It presents a perspective that acknowledges systems to be a set of components that are all interrelated, and where these interrelationships are equally important as the components themselves (Monat & Gannon, 2015). Complex systems are not necessarily systems with a large scale. The Bajeskwartier water system can also be seen as a complex system where system thinking can be useful in understanding the system dynamics of the water balance. Several key elements from the systems thinking theory (Arnold & Wade, 2015) will be used in the research methods:

1. Differentiating stocks, flows, and variables
2. Gaining insight into non-linear relationships
3. Become aware of the dynamic behavior

By assessing the Bajeskwartier water system as a complex system and using these key elements, a deep understanding can be created of the behavior of the system. When an understanding of the drivers of the system is gained, consideration can be made to which parts of the water system are fundamental processes that will lead to the design of the digital representation. Additionally, an iterative approach to systems thinking will be implemented in this research. By analyzing the output of the optimization model, underlying relationships between model components can be understood on a more complex level. When different scenarios are tested, the dynamic behavior of the system will become visible. Using this knowledge, the model will then be further improved to increase its accuracy.

2.2 Scenario planning

Scenario planning is a technique that can combine multiple scenarios to present a variety of future projections (Star et al., 2016) and has proven to be an effective way to plan for climate adaptation (Lawrence et al., 2021). In scenario planning, a set of scenarios that are divergent, plausible, and challenging are used to cover the full spectrum of possible futures (Star et al., 2016). Decision makers can test (climate change mitigation) plans with these scenarios to assess whether unforeseen problems might arise in the future. For the Bajeskwartier case, scenario planning will be used in two ways. First, climate change scenarios will determine the intensity of the drought period to test the Bajeskwartier drought resilience. Secondly, various scenarios for the local vegetation types will be created to test the behavior of the water system model.

Climate change forecasts are an important source of information for governance institutions to assess the implications that climate change can have (Star et al., 2016). However, predicting the future climate is difficult due to the complexity of the system. With the current modeling techniques, there will always be a level of uncertainty in the projections (Star et al., 2016). Although planning for a single, most likely climate change projection appears to be the most straightforward and time-effective planning method, implementation of various scenarios enhances the robustness of the planning process by including the uncertainties that a single scenario cannot do (Lawrence et al., 2021).

2.3 Optimal water resource allocation

Allocation optimization of available water is important in times when the resources are limited (D. Liu et al., 2018). As mentioned, it is expected that periods of prolonged rainfall deficit will occur more frequently and severely due to the changing climate (Seneviratne et al., 2021). This can result in a situation where the water availability for the green infrastructure in the Bajeskwartier drops below the water stress threshold. When water resources are optimally allocated, this can be delayed or prevented. In the optimization of water resources, objective functions are set as well as constraints to set limits and boundaries for the dynamics of the model (D. Liu et al., 2018). Constraints can be limits on economic costs, pumping capacity, limitations on the use of potable water, among others. Governmental policies can be modeled by the adaptation of objective functions and constraints. In such optimization analyses, scenario planning can be implemented in terms of climate change scenario analyses, as well as scenarios where different vegetation types are explored.

2.4 Theory integration

The three theories act as the foundation on which the methods will be based. In Figure 2.2, a visual representation is presented of which sections of the methods are based on which theory. The squares with 3.1 to 3.7 represent the sections in the methods chapter. Additionally, for each theory, the relevant sub-research questions are displayed.

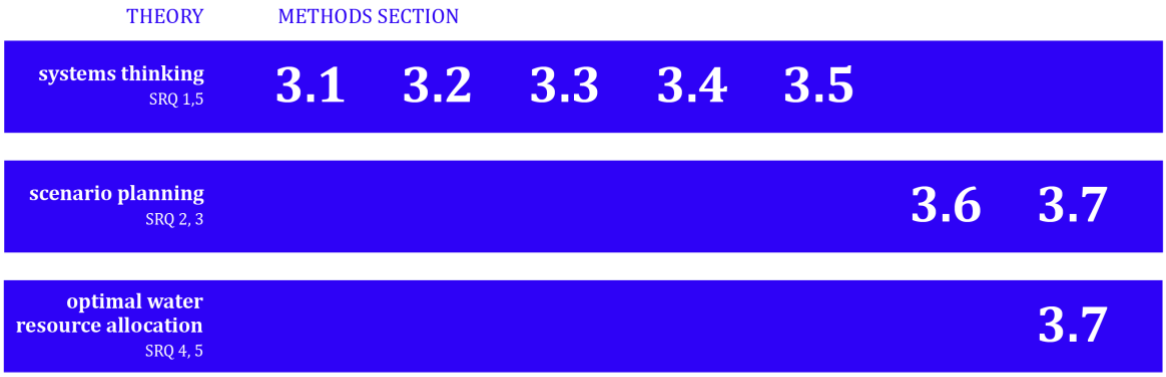

Figure 2.2: visual representation of the theory integration in the methods and sub research questions

3. Methods

To assess the drought resilience and optimal water resource management for the Bajeskwartier, several steps will be taken. First, the physical aspects of the area will be explored (section 3.1). Secondly, the flows in and out of the soil moisture balance equation will be defined, including an explanation of the deep percolation and runoff processes (section 3.2). Subsequently, an evapotranspiration module for the model will made to generate vegetation water use from the climate data (section 3.3). Lastly, to complete the formulation of the soil moisture balance flows, the groundwater contribution process will be dissected (section 3.4).

After this theoretical basis has been set, the remaining input data for the model will be gathered in sections 3.5 and 3.6. First, site-specific soil and vegetation characteristics for the Bajeskwartier are explored (section 3.5). Hereafter, the input data will be completed by assessing climate scenarios created by the KNMI weather institute (section 3.6). Various climate change scenarios will be investigated and a one-year weather simulation with an extreme drought will provide climate data.

The last step of the methodology is to combine the theoretical section and the local conditions in an optimization solver environment to model different scenarios for the Bajeskwartier water management (section 3.7).

3.1 Bajeskwartier water system

The Bajeskwartier is an urban area located in the Venserpolder, in the east of Amsterdam. Due to the location in a polder, the ground surface is 0.8 meters below sea level. In Figure 3.1, a schematic layout of the neighborhood is displayed with the distinction between unpaved surfaces (greenspace), paved surfaces, buildings, and zonal division. The neighborhood has a rectangular shape with large green areas between the buildings. There will be various functions for the greenspace with a wide range of vegetation types. Additional green space is planned as green roofs on the buildings. These can benefit rainwater buffer capacity and provide additional public space on the roofs. However, for this research the assumption will be made that all green areas have the same properties and green roofs will not be included. This is to prevent the model from becoming too complex. When this first version of the model is complete, a more detailed representation of the green spaces can be added.

There will be large areas of open surface water in and around the Bajeskwartier. Surrounding the neighborhood is the old prison moat which will be connected with several

ponds. These provide climate-adaptive properties such as rainwater runoff areas and active cooling in times of extreme heat.

Figure 3.1: Bajeskwartier layout with zones (Angou et al., 2022)

As seen in Figure 3.1, the Bajeskwartier is separated into eight different zones, which have one or multiple buildings and an area of greenspace. Underneath the buildings, in the crawling spaces, there will be buffer capacity created for rainwater. This is to alleviate the pressure on the local sewer systems in case of heavy rainfall events. However, these spaces can also be adapted to provide rainwater storage to use for irrigation in prologued droughts. Rainwater can be harvested from the roofs by connecting the storage tanks to a regular drainage system. Per zone, the m^2 of greenspace, m^3 of potential water storage, and m^2 of rainwater collection area are shown in Table 3.1.

Table 3.1: area of greenspace per zone in the Bajeskwartier, the m^3 of water storage space under the buildings and roof area where water can be collected per zone.

Zone	**Greenspace [m^2]**	**Water storage [m^3]**	**Rainwater collection area [m^2]**
1	1898	476	1992
2	782	305	424
3	1583	863	1904
4	1389	1084	1506
5	2214	1080	3132
6	1437	1151	1598
7	1558	868	5056
8	5657	3809	6265
Total	16518	9636	21877

3.2 Soil moisture balance

The soil moisture content in the rootzone is the metric that will be used to determine the water availability for the vegetation in the Bajeskwartier. Soil moisture content can be derived from the rootzone soil moisture balance. A moisture balance is a balance between all flows in and out of a soil. Precipitation, runoff, irrigation, evapotranspiration, deep percolation, and groundwater contribution are soil water flows that determine the soil moisture content in the rootzone (θ) (Pereira & Alves, 2005). The equation (3.1) calculates the θ (Pereira & Alves, 2005).

$$\theta_{z,t} = \theta_{z,t-1} + \frac{P_t - RO_{z,t} + I_{z,t} - ETa_{z,t} - DP_t + GC_{z,t}}{zr} \quad z \in Z, t \in T \qquad (3.1)$$

Formula (3.1) is indexed per zone and time, where Z refers to the set of zones z, and T refers to the set of time instances t. P_t is the precipitation [mm], $RO_{z,t}$ is the runoff [mm], $I_{z,t}$ is the irrigation [mm], $ETa_{z,t}$ is the actual evapotranspiration [mm], $DP_{z,t}$ is the deep percolation [mm], $GC_{z,t}$ is the groundwater contribution [mm], and zr is the rooting depth [mm]. Runoff is the process where excess water drains from the soil when the soil is saturated, as explained in section 3.7.2. Evapotranspiration will be explained in depth in section 3.3. Groundwater contribution is the upwards flow from deeper groundwater to the rootzone, and will be highlighted more extensively in section 3.4. Deep percolation is the process of downward water drainage from the rootzone to deeper soil layers, as shown in formula (3.2) (Pereira & Alves, 2005).

$$DP_{z,t} = 0 \; when \; \theta_{z,t} \leq \theta fc \; otherwise \; DP_{z,t} = (\theta_{z,t} - \theta fc) zr \quad z \in Z, t \in T \qquad (3.2)$$

Deep percolation takes place when the soil moisture content is higher than the field capacity (θ_{FC}) (Y. Liu et al., 2006). The field capacity represents the moisture content value which remains after all excess water has been drained from the soil and the downward flow is stagnated (Rai et al., 2017). At this point, the gravitational force is equal to the force that keeps the moisture in the soil.

3.3 Evapotranspiration

Crop evapotranspiration is used as a way of assessing how the water requirement of vegetation is affected by local climate conditions (Allen et al., 1998). Evapotranspiration consists of two separate processes: evaporation and transpiration. As these processes take place at the same time and distinction between the two is difficult, they are combined in a single metric. In the process of evaporation, energy from solar radiation and ambient air temperature cause water molecules on surfaces to turn from liquid into vapor (Allen et al., 1998). Additionally, air humidity and wind speeds influence the rate of evaporation. Evaporation occurs from surfaces such as open water, soils, and pavements.

Transpiration is the process where plants release water vapor from the stomata in the leaves (Allen et al., 1998). Plants use water to transport nutrients from the soil to different parts of the plant and close to all water taken up by the roots is later released through the stomata. The climatic conditions which affect the evaporation rate also drive the transpiration process. In addition to these conditions, soil characteristics such as soil type and soil moisture content, as well as plant characteristics influence transpiration.

3.3.1 Penman-Monteith

To estimate the water use of the Bajeskwartier greenspace, the evapotranspiration will be calculated. By calculating the reference evapotranspiration (ET0), a baseline amount can be set to which complexity can be added. ET0 uses standardized homogenous vegetation that has a close resemblance to a grass field, and there is always sufficient soil moisture (Allen et al., 1998). To calculate the ET0, the Penman-Monteith equation from formula (3.3) will be used (Angou et al., 2022).

$$ET0_t = \frac{1}{\lambda} \frac{e's\ Rn + \frac{Cp\ \rho\alpha}{ra}(es - ea)}{e's + \gamma\left(1 + \frac{rs}{ra}\right)} \qquad t \in T \tag{3.3}$$

In formula (3.3) the latent heat of vaporization (λ) is set to a fixed value of 2.45 MJ/kg, σ is the Stefan-Boltzmann constant (4.903 * 10^{-9} MJ/m^2/°K^4/day), Cp is the specific heat of moist air (0.001013 MJ/kg/°C), ρα is the air density (1.2 kg/m^3), γ is the psychometric constant (0.067 kPa/°C), and rs is the fixed surface resistance. The reference vegetation for ET0 is assumed to have a surface resistance of 70 s/m ($\frac{70}{86400}$ day/m) (Allen et al., 1998). The remaining values for the ET0 formula can be calculated with the formulas (3.4) to (3.10).

$$es = 0.6108e^{\frac{17.27T}{273.3+T}} \tag{3.4}$$

$$e's = \frac{4098es(T)}{(237.3 + T)^2} \tag{3.5}$$

$$ea = \frac{RH}{100}es \tag{3.6}$$

$$Rn = Rns - Rnl \tag{3.7}$$

$$Rns = (1 - \alpha)\left(0.25 + 0.5\left(\frac{n}{N}\right)\right)Ra \tag{3.8}$$

$$Rnl = \left(0.9\left(\frac{n}{N}\right) + 0.1\right)\left(0.34 - 0.14\sqrt{ea}\right)\sigma(T + 273.2)^4 \tag{3.9}$$

$$ra = \frac{208}{86400u} \tag{3.10}$$

In formula (3.4), the saturation vapor pressure (es) [kPa] is calculated, where T is the mean daily air temperature at 2m height [°C]. Formula (3.5) defines the change of es with T. The actual vapor pressure (ea) will be calculated with formula (3.6), where RH is the relative humidity [%]. The net radiation (Rn), formula (3.7), is the difference between the net incoming solar radiation (Rns), formula (3.8), and the net outgoing longwave radiation (Rnl), formula (3.9). In formulas (3.8) and (3.9), α is the albedo coefficient, n is the hours of bright sunshine [h], N is the total hours of sunlight [h], and Ra is the solar radiation at the top of the atmosphere [W/m^2]. The reference vegetation has an albedo coefficient of 0.23 (Allen et al., 1998). In formula (3.10), the aerodynamic resistance (ra) is calculated, where u represents the wind speed [m/s].

3.3.2 Adjustment factors

ET_0 assumes that there is optimal soil moisture, perfect management, and ideal environmental conditions, combined with a standardized crop (Allen et al., 1998). By including adjustment factors, transformations can be made to ET_0 to obtain evapotranspiration values that are closer to reality. Vegetation and soil moisture specific adjustment factors will be applied to the ET_0 to obtain the actual evapotranspiration (ET_a) (Zeleke & Wade, 2012). ETa is a combination of the ET0, the crop factor (Kc), and a soil water stress coefficient (Ks) (Zeleke & Wade, 2012). Formula (3.11) will be used to calculate the ET_a.

$$ETa_t = ET0_t\ Kc\ Ks_{z,t} \qquad z \in Z, t \in T \tag{3.11}$$

The Kc is a dimensionless value that transforms the ET0 to vegetation specific evapotranspiration (Allen et al., 1998). K_c integrates the difference in vegetation characteristics

compared to the reference crop into a single factor (Allen et al., 1998). Crop type, variety, and development stage affect the value of K_c. Additionally, the soil water balance influences the available water for the vegetation and thus affects evapotranspiration rates. When the soil moisture content in the rootzone drops below the threshold moisture content (θa), the evapotranspiration amount will decrease due to plant stress (Zeleke & Wade, 2012). In the ETa formula, this decrease in evapotranspiration is accounted for with the soil water stress coefficient Ks. A visual representation of Ks is shown in figure 3.2.

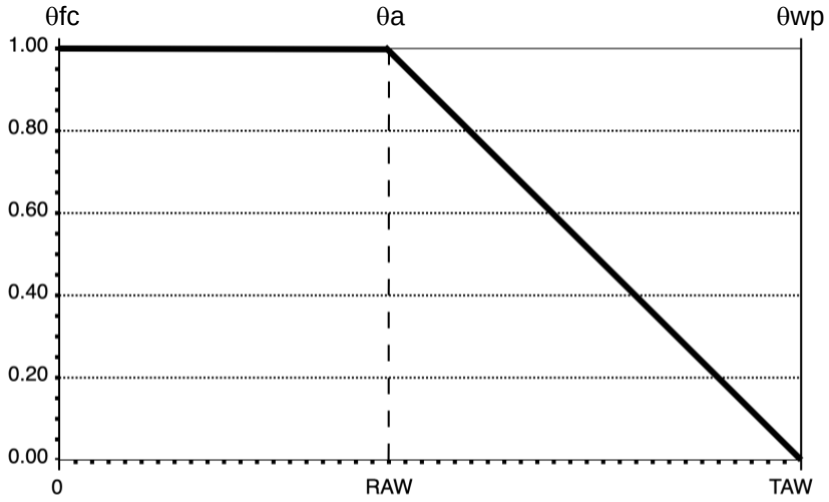

Figure 3.2: Visual representation of Ks (Zeleke & Wade, 2012)

The field capacity (θfc), wilting point (θwp), and θa determine the way vegetation responds to varying moisture content values in the rootzone. As mentioned earlier, the moisture content at field capacity is the most optimal for plant growth and plant stress occurs when the moisture content is lower than the threshold moisture content. When the soil moisture content decreases even more and reaches the wilting point, the roots can no longer extract water from the soil and vegetation will start wilting. To calculate θfc and θwp, respectively, formulas (3.12) and (3.13) will be used (Angou et al., 2022).

$$\theta fc = \theta r + (n - \theta r)\left(\frac{\psi b}{10^2}\right)^{\lambda} \tag{3.12}$$

$$\theta wp = \theta r + (n - \theta r)\left(\frac{\psi^b}{10^{4.2}}\right)^{\lambda} \tag{3.13}$$

In (3.12) and (3.13) θr is the irreducible moisture content, n is the porosity, ψb is the displacement pressure, and λ is the pore size distribution index. Local soil properties determine the irreducible moisture content, porosity, displacement pressure, and pore size distribution index (Van Genuchten et al., 1991). With the θfc and θwp, θa will be calculated using formula (3.14) (Angou et al., 2022).

$$\theta a = (1 - p)\theta fc + p\theta wp \tag{3.14}$$

Here, p is the depletion factor. This factor is dependent on the site-specific vegetation type. In section 3.5.1 of the Bajeskwartier case study, the soil and vegetation properties will be elaborated in further detail.

After determining the θfc, θwp, and θa, a conditional statement for Ks can be derived from the water stress coefficient graph in figure 1. When the soil moisture content at a certain day (θi) drops below θa, Ks starts to decline linearly until it reaches zero at the wilting point. As Ks cannot be a negative value, a bound is set in the model. This conditional statement will be shown in the Bajeskwartier case study chapter.

3.4 Groundwater contribution

The soil moisture balance method of Pereira and Alves (2005) does not give a detailed way to determine the groundwater contribution (GC), also known as capillary rise. Therefore, an addition to the soil moisture balance formula has been made to include a more comprehensive method to calculate the GC. An approximation of the GC [mm/day] is calculated using formula (3.15) (Y. Liu et al., 2006).

$$GC_{z,t} = \begin{cases} Gmax_t, & when\ W < Ws \\ Gmax_t\left(\dfrac{Wc - W}{Wc - Ws}\right), & when\ Ws \le W \le Wc \\ 0, & when\ W > Wc \end{cases} \qquad z \in Z, t \in T \qquad (3.15)$$

In formula (3.15), Gmax is the steady upward flux [mm/day] and represents the potential maximum upward flow from the groundwater to the rootzone per day. W is the actual soil water storage in the root zone [mm] and is derived from θ, Wc is the critical water storage [mm], and Ws is the steady soil water storage [mm]. Whether the Gmax is reached depends on the soil water storage. The GC formula is accompanied by formulas (3.16) to (3.20) to calculate Wc, Ws, and Gmax (Y. Liu et al., 2006).

$$\mathrm{Wc} = \mathrm{a1Dw}^{\mathrm{b1}} \qquad (3.16)$$

$$\mathrm{Ws} = \mathrm{a2Dw}^{\mathrm{b2}} \qquad (3.17)$$

$$\mathrm{Dwc}_t = \begin{cases} \mathrm{a3ET0}_t + \mathrm{b3}, & when\ \mathrm{ET0}_t \le 4mm/day \\ 1.4, & when\ \mathrm{ET0}_t > 4mm/day \end{cases} \qquad t \in T \qquad (3.18)$$

$$\mathrm{Gmax}_t = \begin{cases} k\mathrm{ET0}_t, & when\ \mathrm{Dw} \le \mathrm{Dwc}_t \\ \mathrm{a4Dw}^{\mathrm{b4}}, & when\ \mathrm{Dw} > \mathrm{Dwc}_t \end{cases} \qquad t \in T \qquad (3.19)$$

$$k_t = \begin{cases} 1 - e^{-0.6LAI}, & when\ \mathrm{ET0}_t \le 4mm/day \\ 38 / \mathrm{ET0}_t, & when\ \mathrm{ET0}_t > 4mm/day \end{cases} \qquad t \in T \qquad (3.20)$$

Gmax is mainly determined by the groundwater depth (Dw) and the ET0, which in this case represents the evaporative demand (Y. Liu et al., 2006). The critical groundwater depth (Dwc) acts a threshold value for the Dw and sets a breakpoint above which Gmax remains constant (Y. Liu et al., 2006). The k factor is used to convert ET0 into the potential crop transpiration. The leaf area index (LAI) is the coverage of the vegetation relative to the unit ground surface area (Bréda, 2003). To complete the calculations, the parameters a1 – a4, b1 – b4, and the LAI must be set and defined by assessing local soil properties. For the Bajeskwartier case study, the chosen values for the parameters are explained in the next chapter.

3.5 Bajeskwartier case study

After determining how to calculate the evapotranspiration and soil moisture balance, the local Bajeskwartier conditions will be studied to obtain case study data to test the model. In an area that is still under development, soil properties are likely to change from the current state until the project is completed. Therefore, some approximations are made for the soil and vegetation properties to obtain values that are currently unknown.

3.5.1 Soil and vegetation characteristics

To calculate θfc, θwp, and θa, one needs the irreducible moisture content, porosity, displacement pressure, and pore size distribution index. These are determined by local soil conditions. The Living Lab expert report on a proposed functional design considered local sources and Bajeskwartier experts to get insight into how the soil will be created and in what properties that will result (Angou et al., 2022). They determined an irreducible moisture content of 0.07, a porosity of 0.41, a displacement pressure of 12 cm, and a pore size distribution index of 0.26 (Angou et al., 2022).Currently, these approximations are the most accurate and will be used in this Bajeskwartier drought resilience analysis.

Rooting depth and depletion factor depend strongly on the vegetation type. A deep rooting depth can contribute to higher drought resilience of vegetation and varies per plant species (Fan et al., 2017). For the standardized vegetation corresponding to the reference evapotranspiration, the rooting depth is 500 mm, and the depletion factor is 0.5 (Allen et al., 1998). When running different model scenarios, the rooting depth can be changed to assess how different plant characteristics affect the system behavior.

3.5.2 Adjustment factors

As mentioned in the evapotranspiration section of the methodology, the Kc and Ks are used to obtain the ETa of the Bajeskwartier. Kc is defined by the vegetation present in the study area. For the Bajeskwartier area, a wide range of vegetation types have been proposed by the landscape architects (AM & Fabrications, 2020). Currently, the first version of the drought resilience model uses the reference crop as a baseline, with a corresponding Kc of 1.0. This will be changed when the scenario analysis of the different vegetation characteristics is performed. Changing the Kc is an effective way to test the sensitivity of the model when the first version is proven to be working.

Using the soil and vegetation characteristics, the field capacity, wilting point, and threshold moisture content will be calculated. Afterwards, the equation for Ks will derived by taking the Ks = 1 point with the corresponding θa of 0.194, and the Ks = 0 point with a corresponding θwp value of 0.122. The conditional statement in formula (3.12) was derived when combining the resulting equation and the fact that the Ks is equal to 1 when the moisture content is higher than the threshold moisture content.

$$\mathrm{Ks}_{z,t} \begin{cases} 1, & if\ \theta_{z,t} \geq \theta a \\ 13.89\theta_{z,t} - 1.70, & otherwise \end{cases} \qquad z \in Z, t \in T \tag{3.21}$$

3.5.3 Groundwater contribution parameters

Under certain conditions where the groundwater is close to the bottom of the rootzone, the upward water flow from the groundwater to the rootzone can provide up to 41% of the water used by vegetation (Gao et al., 2017). The groundwater in the Bajeskwartier is 2.5 meters below NAP and is kept constant due to the area being a polder (Angou et al., 2022). With a ground level of 0.8m below NAP, a constant groundwater level of 1.7m below the ground level is

considered (Angou et al., 2022). According to Gao et al. (2017), this is regarded as sufficiently close to the rootzone to have a significant effect on the soil water balance.

To perform the GC calculations on the Bajeskwartier case, parameters a1 to a4 and b1 to b4 must be set. An approximation method is given by Liu et al. (2006) to determine parameter values. Parameters a1 to a3, b1, and b2 are straightforward to set. For a1 and a2, the soil water storage to 1.0-meter depth at the field capacity and wilting point will be used, which are determined by multiplying the θfc and θfc by 1000. Parameters b1, b2, and a3 will be constant values for every type of soil. For parameters b3, a4, and b4, local soil properties will be needed to determine the values. Currently, the Bajeskwartier is still in the construction phase so no specific soil characteristics of how the soil will be are available. Therefore, the soil properties of the current data provided by the engineering firm Sweco will be used as a guide to set the parameters (Sweco, 2020). They conclude that currently, the soil has loamy sand characteristics. Knowing this, the corresponding values for b3, a4, and b4 can be chosen according to the guidelines set by Liu et al. (2006). This results in the following parameter values:

$$\mathrm{a1} = z^r \theta^{FC};\ \mathrm{b1} = -0.17$$
$$\mathrm{a2} = 1.1\big((\mathrm{zr}\,\theta\mathrm{fc}) + (\mathrm{zr}\,\theta\mathrm{wp})\big)/2;\ \mathrm{b2} = -0.27$$
$$\mathrm{a3} = -1.3;\ \mathrm{b3} = 6.2$$
$$\mathrm{a4} = 3;\ \mathrm{b4} = -2.5$$

The final constant that must be set to calculate groundwater contribution is the leaf area index (LAI). A value of 2.5 will be set currently to correspond to the reference vegetation characteristics (Scurlock et al., 2001).

3.6 Climate scenario

Climate change scenarios from the IPCC are based on the change of greenhouse gas (GHG) concentrations over time (IPCC, 2013). These GHG concentration scenarios are expressed as Representative Concentration Pathways (RCP). To translate these RCP climate change scenarios into high-resolution local weather data, stochastic weather generators are used to generate time series simulations of weather (J. Chen & Brissette, 2014). These models create precipitation, temperature, solar radiation, wind, and other meteorological data based on historically observed weather time series of the desired location (Ailliot et al., 2015).

To study the impact of extreme droughts, consideration must be taken to obtain suitable weather data simulations. The KNMI provides comprehensive datasets of meteorological data, including data with transformations to predict climate conditions under certain IPCC climate change scenarios. A record of daily precipitation, temperature, and solar radiation measurements from 1980 until 2010 has been transformed according to three different climate change scenarios (Van Den Hurk et al., 2014). This dataset was created in 2014 with scenarios from that time. Therefore, the most extreme KNMI scenario will be chosen for this research. The nearest KNMI weather station to the Bajeskwartier is located at the Hortus Botanicus in Amsterdam (station 441) and measures only precipitation. Temperature and solar radiation will be obtained from the Schiphol weather station (station 240). Besides precipitation, temperature, and solar radiation, additional weather data will be needed to calculate evapotranspiration. Wind speed, hours of sunlight, hours of bright sunshine, and relative humidity will be retrieved from historical data from the Schiphol weather station.

After combining and cleaning the datasets, an analysis is performed to determine the number of consecutive days with precipitation lower than 0.1 mm. A minimum temperature was set at 15 degrees Celsius to omit dry periods in the colder months. The analysis resulted in

the year 1995 coming up as the year with the most extreme summer drought. From this point onwards, the year 1995 will be used as input data for the Bajeskwartier model simulations.

3.7 Optimization

A digital representation of the water balance will be implemented in a Pyomo optimization environment. The model will be built up with the eight Bajeskwartier zones where the greenspace, water storage facility, and water collection area on buildings are defined. Within a zone, the soil moisture balance will be defined with the associated in- and outflows. Additionally, there are flows from the water collection on the roof to the water storage, and from the storage to the irrigation system. Subsequently, the irrigation will be one of the inflows of water into the soil moisture balance.

After the theoretical background is defined and the relevant data is gathered, several soil processes will be calculated and used as additional input data for the optimization. Hereafter, the optimization formulation will be presented and the scenarios which will be tested with the model will be defined.

3.7.1 Input data

To reduce complexity in the optimization problem, several processes are calculated beforehand and are used as input data. Figure 3.3 shows a visual representation of the preprocessing stage which leads to the input data for the optimization. First, the reference evapotranspiration will be calculated according to the extreme drought year defined in the previous chapter. As ET0 is not different per zone, it can be calculated beforehand. Additionally, θfc, θwp, and θa from formulas (3.12) to (3.14), and the groundwater contribution parameters will be input data to the model. These parameters will then be used to calculate the Wc, Ws, Dwc, Gmax, and k with formulas (3.16) to (3.20). These variables use ET0 and are not different per zone and can therefore be calculated beforehand. This reduces the complexity of the optimization by calculating a nonlinear variable as input data and therefore enhancing model performance.

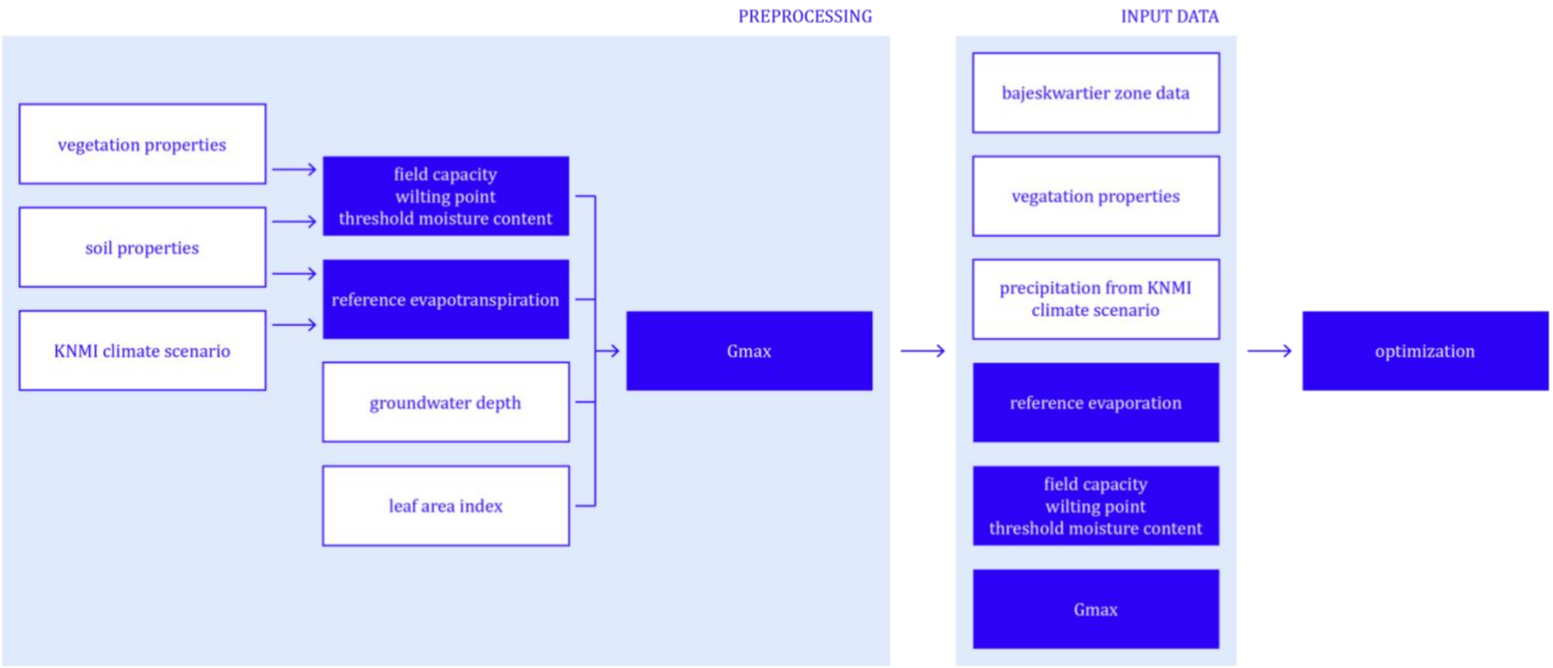

Figure 3.3: flowchart of the preprocessing and input data for the optimization problem

3.7.2 Problem formulation

In the optimization model, the problem is mathematically formulated in formula (3.22) to (3.34). The objective is defined as minimizing the storage capacity per zone in the Bajeskwartier, as well as minimizing the irrigation amount per day per zone.

$$min \sum_{z \,\epsilon\, Z} S\_cap_z + \sum_{z \in Z, t \in T} I_{z,t} \tag{3.22}$$

s.t.

$$(3.1), (3.2), (3.15), (3.21) \tag{3.23}$$

$$RO_{z,t} = \begin{cases} \geq 0, & if\ \theta_{z,t} \geq \theta s \\ 0, & otherwise \end{cases} \qquad z \in Z, t \in T \tag{3.24}$$

$$W_{z,t} = \theta_{z,t}\, z^r \qquad z \in Z, t \in T \tag{3.25}$$

$$V_{z,t} = V_{z,t-1} + Qrt_{z,t} - Qti_{z,t} \qquad z \in Z, t \in T \tag{3.26}$$

$$V_{z,t} \leq storage\_cap_z \qquad z \in Z, t \in T \tag{3.27}$$

$$Y_{z,t} = \frac{A_z \times e \times h_t \times \eta \times 0.05}{1000} \qquad z \in Z, t \in T \tag{3.28}$$

$$Qrt_{z,t} \leq Y_{z,t} \qquad z \in Z, t \in T \tag{3.29}$$

$$Qti_{z,t} = \frac{I_{z,t}\, A_z}{1000} \qquad z \in Z, t \in T \tag{3.30}$$

$$S\_cap_z \geq V_{z,t} \qquad z \in Z, t \in T \tag{3.31}$$

$$\theta a \leq \theta_{z,t} \leq \theta s \qquad z \in Z, t \in T \tag{3.32}$$

$$0 \leq Ks(z,t) \leq 1 \qquad z \in Z, t \in T \tag{3.33}$$

$$I_{z,t} \leq 20 \qquad z \in Z, t \in T \tag{3.34}$$

Z refers to the set of zones z that are defined in chapter 3.1.1, and T refers to the set of time instances t that represent 1-day intervals.

As mentioned, the objective function (3.22) is to minimize the maximum storage capacity needed for each zone (S_cap_z) and the irrigation amount per zone per day ($I_{z,t}$). Constraint (3.23) adds the soil moisture content, deep percolation, actual evapotranspiration, and groundwater contribution formulas to the optimization model.

Constraint (3.24) defines the runoff ($RO_{z,t}$) to be higher than zero when the $\theta_{z,t}$ is higher than the soil saturation level (θs), and otherwise to be zero. Constraint (3.25) transforms the moisture content to the actual soil water storage ($W_{z,t}$) as the product of the moisture content and the rootzone. Constraint (3.26) sets the volume in the water storage tank ($V_{z,t}$) [m^3] as the sum of the previous day $V_{z,t}$ and the flow from the roof to the storage ($Qts_{z,t}$) [m^3] minus the flow from the storage to the irrigation system ($Qtiz_{,t}$) [m^3]. The maximum storage capacity per zone ($storage\_cap_z$) is set as an upper bound to $V_{z,t}$ in constraint (3.27).

How much rainwater can be collected depends on the amount of rainfall, collection area, yield coefficient, and hydraulic filter efficiency (Ward et al., 2012). In constraint (3.28), the maximum potential daily rainwater yield ($Y_{z,t}$) [m^3] is defined as the product of the collection area (A_z) [m^2], yield coefficient (e) [%], rainfall depth (h_t) [mm], and the hydraulic filter efficiency (η), multiplied by 0.05 and then divided by 1000. The yield coefficient and hydraulic filter efficiency are unknown, but they can be assumed to both be 0.9 when this is the case (Ward et al., 2012). Subsequently, constraint (3.29) defines $Qrt_{z,t}$ to be less or equal to $Y_{z,t}$. This way, the model can decide at which time the storage tank will be filled with water for irrigation when needed. Irrigation is a free variable and is determined by the model. $Qti_{z,t}$ is

defined in constraint (3.30) to be the product of irrigation (I_z) [mm] and the greenspace area (A_z) [m^2], divided by 1000.

After defining the water balance in the storage tanks, the S_cap_z is defined to be greater or equal to $V_{z,t}$ in constraint (3.31). Because the objective is set to minimize the S_cap_z, this constraint will return the value for when the storage tank per zone wat at the highest volume in the year.

Constraint (3.32) sets the lower bound for $\theta_{z,t}$ at θa, and the upper bound to θs. This lower bound will force the model to prevent plant stress from occurring. The upper bound represents the soil saturation point. Initially, the model will be tested without the irrigation and water storage system implemented. Here, the $\theta_{z,t}$ lower bound will be set at zero to be able to assess the behavior of the water balance section of the model.

Constraints (3.33) and (3.34), respectively, set the bounds Ks to be between 0 and 1, and $I_{z,t}$ to be lower than 20 mm per day. This maximum irrigation amount is set to simulate the physical limitations of an irrigation system.

3.7.3 Scenarios for optimization

Several model scenarios will be run to test the model performance and how it responds to varying vegetation characteristics. The scenarios will be divided between two states of the model, which are shown in figure 3.4. Initially, the soil moisture balance will be tested for the reference vegetation, without the irrigation system implemented. In this non-irrigation state, the response to different vegetation characteristics will be tested as well by altering the Kc and zr values. Hereafter, the rainwater capture, storage, and irrigation system will be added. For this model state, three scenarios with, respectively, the reference vegetation, drought resilient vegetation, and drought sensitive vegetation will be tested.

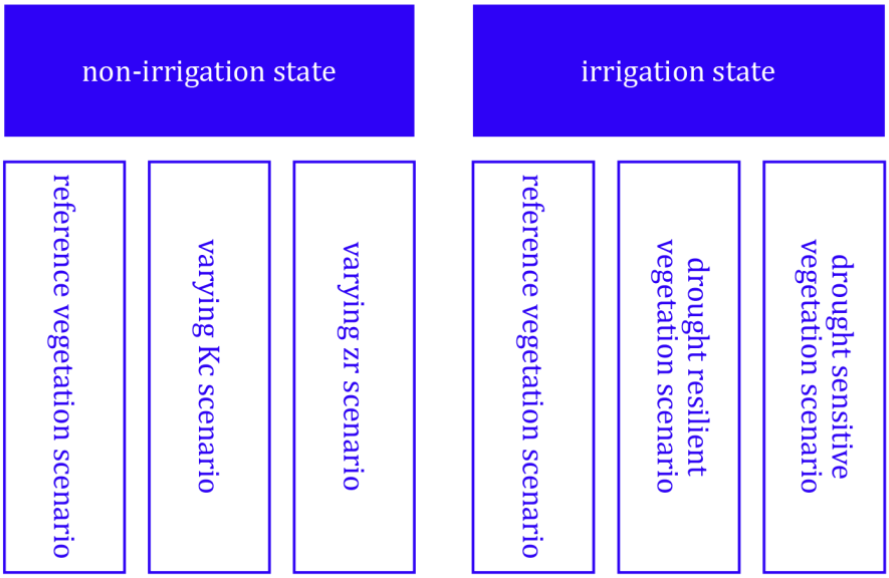

Figure 3.4: scenarios for the optimization problem

In the non-irrigation state of the model, results from the reference vegetation scenario will show how the different processes in the soil respond to a year-long simulation of climate data. This scenario will provide initial insights into how the system responds to an extreme summer drought. Besides, any faults in the implementation of soil processes will become visible and modifications can be made accordingly. Additionally, the response to changing crop

coefficients and rooting depths will be tested in the non-irrigation state of the model. The Kc for the reference vegetation is 1.0 will be compared with a more drought resilient vegetation with a Kc of 0.8 and more drought sensitive vegetation with a Kc of 1.2. These Kc values are determined according to the Food and Agriculture Organization of the United Nations (FAO) guidelines for computing crop water requirements (Allen et al., 1998). Mid-season Kc values range from approximately 0.7 to 1.25 with an average of around 1.1. In the next scenario, three rooting depth values will be tested. The reference vegetation rooting depth is 500 mm, and a deeper rooting depth of 600 mm and a shallower rooting depth of 400 mm will be tested. In the optimization model, the difference between the zones is made through the rainwater capture, storage, and irrigation system. Therefore, the first scenarios are run globally for the Bajeskwartier, without differentiating between the Bajeskwartier zones.

In the irrigation state of the model, the rainwater capture, storage, and irrigation system will be implemented. Simulations will be run with the reference vegetation, drought resilient vegetation (Kc 0.8, zr 600 mm), and drought sensitive vegetation (Kc 1.2, zr 400 mm). These are hypothetical vegetation types based on the expectations that a high Kc and shallow zr result in high water demand, and vice versa. The result from these scenario analyses will be the minimum water storage demand to prevent water stress from occurring in a year with an extreme drought. Additional insights on the irrigation schedule and water storage dynamics will be gained.

3.7.4 Computational considerations

To solve the optimization problem, a Pyomo environment is used in conjunction with disjunctive constraints and a dedicated Mixed-Integer Programming (MIP) solver. In Pyomo, the use of standard if-else statements for variables is not feasible when these are dependent on constraint states (e.g., formula 3.21). This limitation necessitates alternative modeling approaches. To handle disjunctive constraints effectively, the General Disjunctive Programming (GDP) solver GDPOPT will be implemented into the modeling framework (Q. Chen et al., 2022). Additionally, for addressing MIP problems, the GLOA (Globally Optimal Algorithm) algorithm in conjunction with the Gurobi solver will be used (Lee & Grossmann, 2001). On a 2018 MacBook Pro with a 2.3 GHz Intel Core i5 and 8 GB RAM, the average computing time of the optimization problem is approximately four minutes.

4. Results

In this chapter, the results of the Bajeskwartier drought analysis are presented. First, the scenarios regarding the non-irrigation state of the model will be presented in section 4.1. Afterward, the results from the scenarios of the irrigation state of the model will be presented in section 4.2. The input data for the model are shown in Appendix 1.

4.1 Non-irrigation scenarios

The initial model simulations have been made without the irrigation and water storage system. Section 4.1 shows the results of the initial drought stress analysis with the reference vegetation, as well as an analysis of how crop coefficient and rooting depth influence the behavior of the water system.

4.1.1 Drought stress

The results of the baseline reference vegetation scenario are shown in Figure 4.1. Upon first inspection, the model works and shows desirable output. In the top left graph of Figure 4.1, the moisture content is plotted together with the threshold moisture content. The first three months of the year show high moisture content values, suggesting an abundance of precipitation. This is also reflected in the high deep percolation values, as seen in the bottom right graph of Figure 4.1. From approximately the 90th day, the moisture content starts to show larger fluctuations with an overall declining trend. A steep decrease in moisture content starts around day 160 and results in a period of drought stress. As expected, the period where the moisture content is lower than the threshold moisture content corresponds with the summer drought in the KNMI climate simulation. In this optimization scenario, there are 35 consecutive days where the moisture content in the rootzone is lower than the threshold moisture content. This period of drought stress is also shown in the Ks output in the top right graph of Figure 4.1. In theory, the Ks is directly affected by the soil moisture content, so the model shows the desired behavior.

When looking at the groundwater contribution graph in the bottom left of Figure 4.1, a trend can be seen where GC is present at moments where there is a decline in the MC. The highest GC values are present in the summer drought period. These results show that the way GC is modeled resembles the behavior that was expected.

In the period after the drought until the end of the simulation year, MC levels return to a desired range. There are three points visible where there is a steep rise in MC and a large peak in DP. This suggests that in this period precipitation occurs in shorter and more intense peaks than in the beginning of the simulation year. During the whole simulation year, there is no point where the MC reaches the saturation point of 0.41. This means that the runoff remains zero.

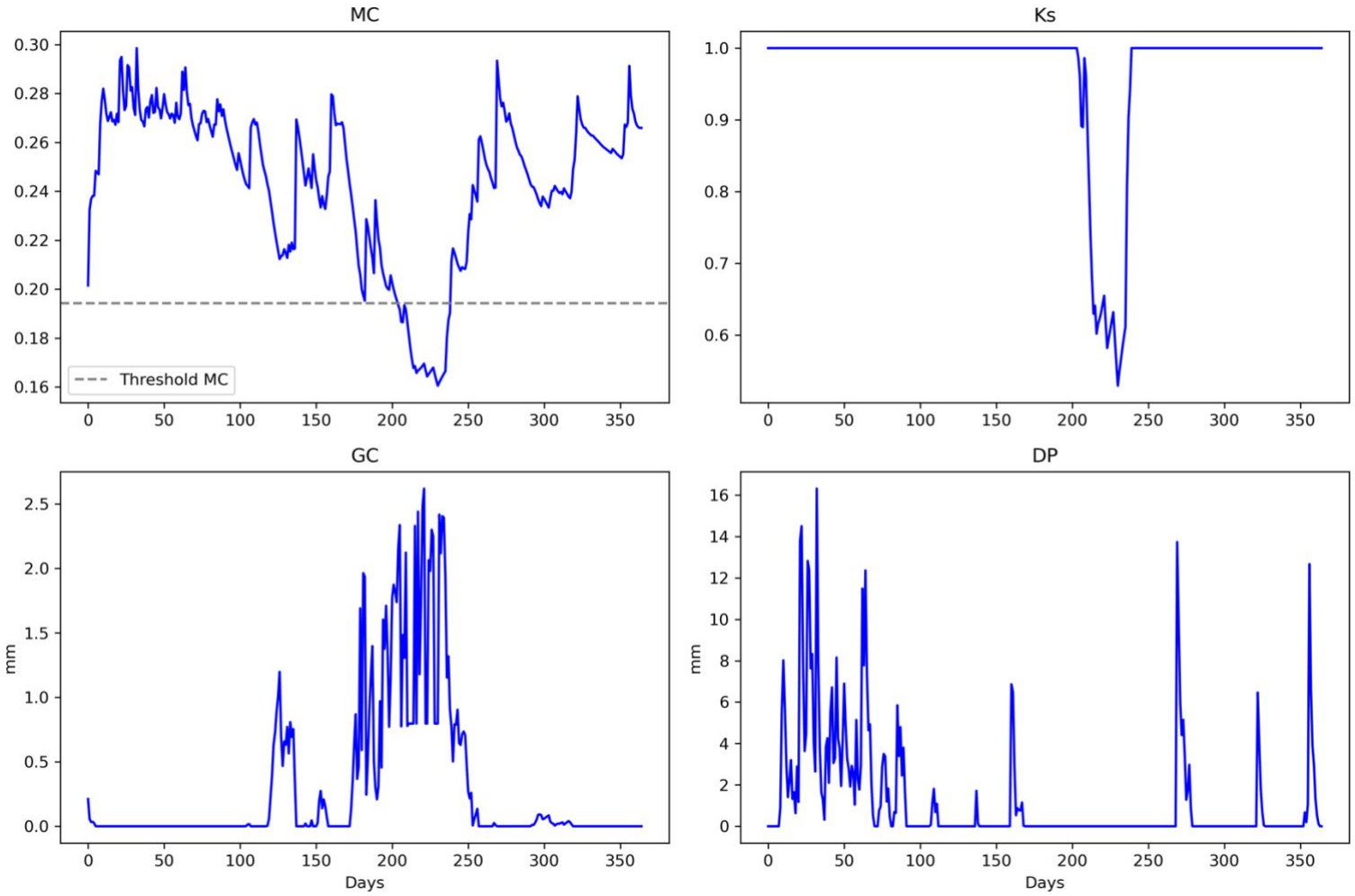

Figure 4.1: Moisture content, K_s, groundwater contribution and deep percolation for the reference crop

Figure 4.2 shows shows the preprocessing output of ET0 and the optimization model output of ETa. Initially, ET0 and ETa overlap, with the blue ET0 line plotted underneath the green ETa line. However, the presence of drought stress is visible in the ETa graph where it deviates from the ET0 line. This period of drought stress corresponds with the Ks graph in Formula 4.1, where the drought stress period is visible from day 200 onwards. ETa is the function of ET0, Ks, and Kc. Consequently, the period where Ks is lower than 1 aligns with when ETa is lower than ET0.

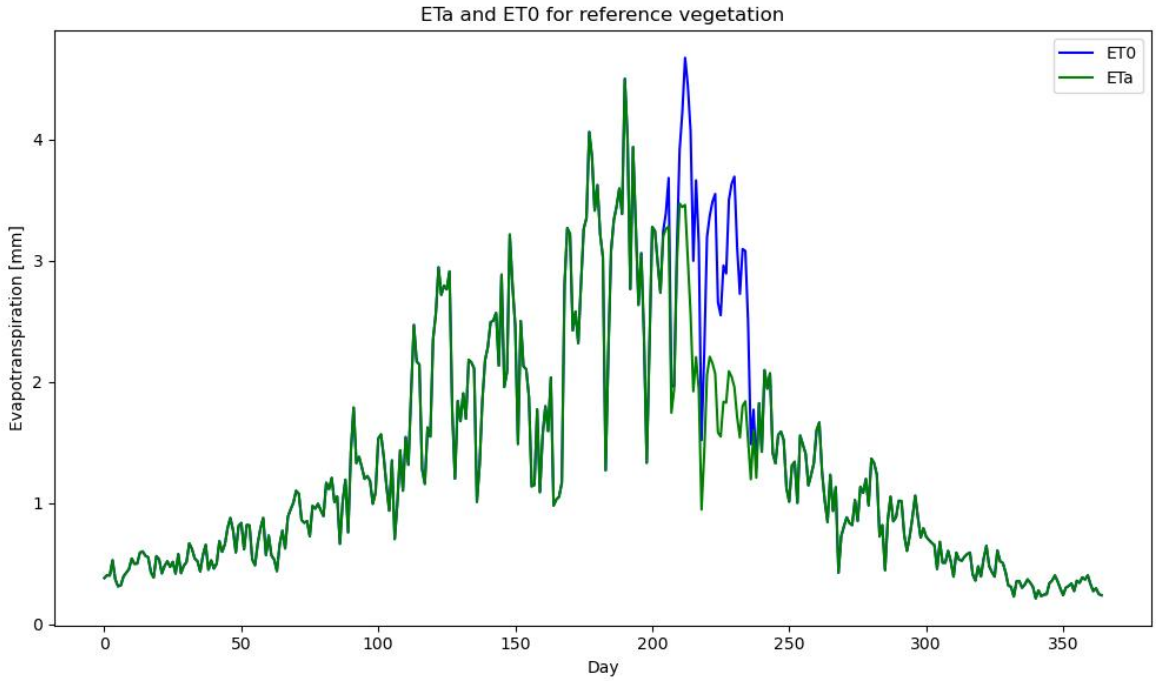

Figure 4.2: the ETa and ET0 for the reference vegetation

4.1.1 Vegetation characteristics

After the baseline soil moisture balance has been set, an analysis was made on the effect of how the Kc and zr affect the behavior of the moisture balance. As mentioned, the model simulation with the reference crop resulted in a 35-day period of drought stress. As seen in table 4.1, for vegetation with a Kc of 1.2 the drought stress days increased to 54. A Kc of 0.8 resulted in 25 drought stress days. There is a large difference in how the Kc influences the amount of drought stress, which is also noticeable in the lowest MC values (Table 4.1). For these simulations, the zr has been kept constant at 500 mm.

Table 4.1: different Kc values and their corresponding number of drought stress days and lowest moisture content values

Kc	**Drought stress days**	**Lowest MC**
0.8	25	0.18
1.0	35	0.16
1.2	54	0.14

Like figure 4.1, Figure 4.3 shows four plotted results for the MC, Ks, GC, and DP for vegetation with Kc 0.8, Kc 1.0, and Kc 1.2. The effect of the different Kc values is most notable in the MC and Ks output. In the first quarter of the year, the MC is relatively stable at a high amount and the different Kc values show similar results. Around day 100, when the MC starts to show larger fluctuations, the MC graphs start to diverge. From this point onwards, the vegetation with Kc 1.2 has the lowest MC and the Kc 0.8 vegetation has the highest MC values. It appears to be the case that the lower the MC is, the larger the difference becomes for the different Kc values. During the drought stress period in the summer, the largest difference in MC values can be observed.

At times where the MC is lower than the threshold MC, the Ks becomes negative. Consequently, a Kc of 1.2 results in the lowest Ks values which is in line with the trend that can be seen in the MC graph. The higher the Kc the lower the MC becomes in the drought

period. Additionally, the length of the period when Ks is below one also increases when the Kc is higher.

For GC, the most apparent difference is visible in the period between day 100 and day 150, near day 250, and around day 300. The simulation with Kc 1.2 shows the highest GC values and the Kc 0.8 simulation the lowest. During the summer drought, from around day 190 onwards, there are high levels of GC, but no clear trend is visible.

In the bottom right graph of figure 4.3, the DP results are shown. During the first quarter of the year where the MC is stable around a high value, the different Kc values only result in small differences in DP. However, later in the simulation year large peaks in DP can be observed where the different Kc values result in more deviations in DP. These peaks all appear after a period where there is no DP, which might cause this difference. In all cases, the lowest Kc results in the highest DP.

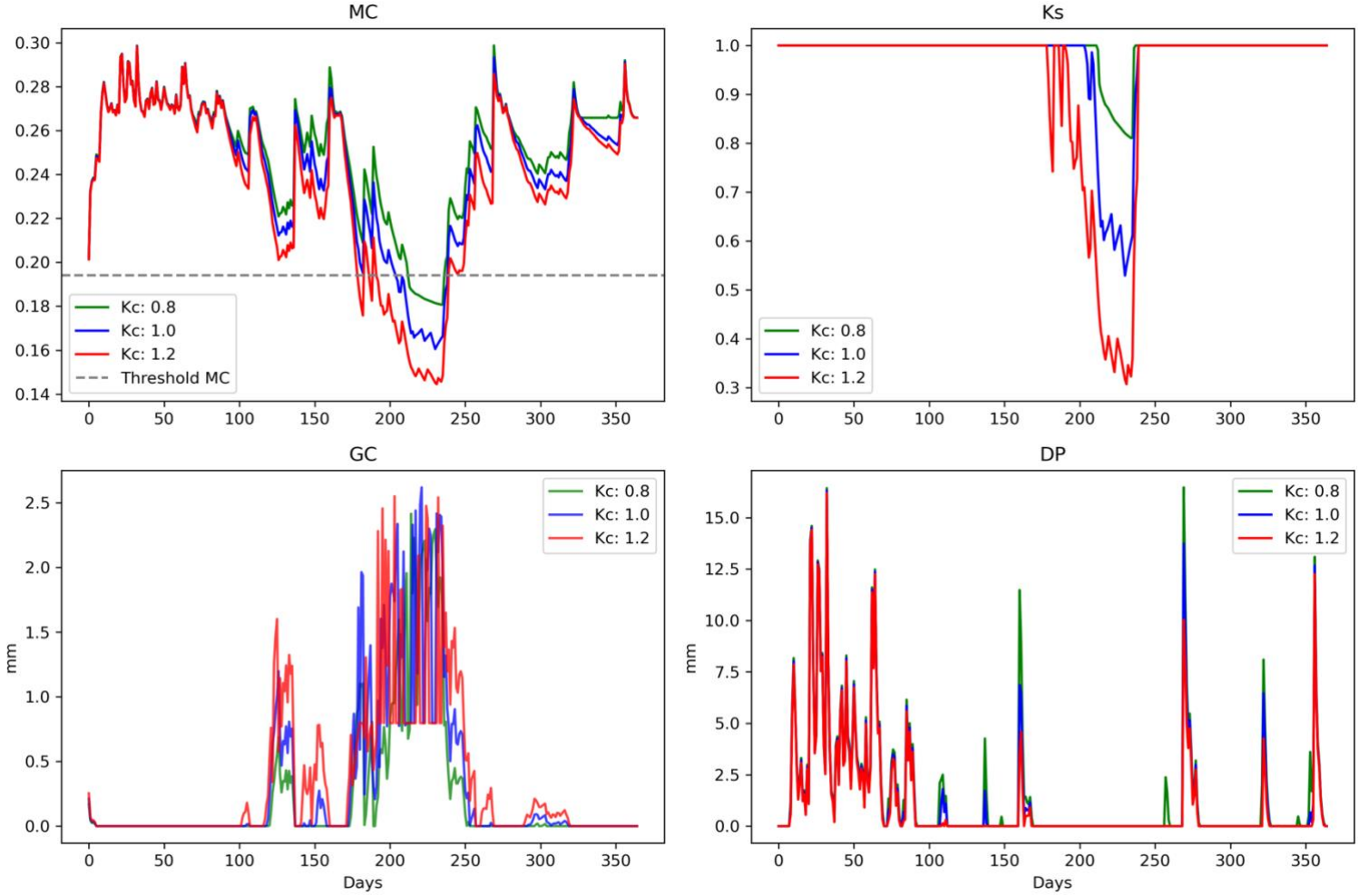

Figure 4.3: Moisture content, Kc, groundwater contribution and deep percolation for different Kc values

In the scenario where the rooting depth is varied, the effect on the amount of drought stress is less notable than the change in Kc values. Table 4.2 shows the number of drought stress days and the lowest MC value for three different zr values. For these simulations, the Kc has been kept constant at 1.0. The reference vegetation zr of 500 mm is the baseline of 35 drought stress days. When decreasing the zr to 400 mm, the number of drought stress days increases to 39. If the zr is deeper, the number of drought stress days decreases to 31. In contrast to changing the Kc, there is only a small difference in the lowest MC values when altering the zr.

Table 4.2 Different zr values and the corresponding number of drought stress days and lowest moisture content values

zr	Drought stress days	Lowest MC
400	39	0.158
500	35	0.160
600	31	0.163

Figure 4.4 shows the difference in MC, Ks, GC, and DP for the three different rooting depths. While the effect of different zr values might seem limited at first glance, there is an interesting result visible in the MC graph. Compared to the other two zr values, the 400 mm rooting depth always shows the highest values at peaks in the MC, but also the lowest values at the troughs of the graph. The opposite behavior can be seen for the 600 mm zr. At the peaks in the graph, it has the lowest MC and at the troughs the highest values. The zr 500 is always the middle value between the other two.

When looking at the Ks results in the top right graph of Figure 4.4, the zr 400 has the lowest Ks values and the zr 600 the highest. This is in line with the result of the MC, where the lowest zr has the most water deficit and the highest zr has the least water deficit.

For the groundwater contribution, it can be seen from the lower left graph in Figure 4.4 that the vegetation with the zr of 400 mm has generally the highest amount of GC. However, in the period where the most drought stress occurs, the groundwater contribution values for the three zr values are close to equal.

When looking at the deep percolation in the bottom right graph of Figure 4.4, a small difference between the different zr values can be observed in several peaks of the graph. At these points, the shallower the zr is, the higher the DP becomes. However, this appears to only be the case when short and sudden peaks in DP occur after a period of no DP. During the first quarter of the year, there is an abundance of water and high DP values. In this period, the DP values for the different rooting depths appear to be equal. This behavior is similar to the DP patterns observed in Figure 4.2.

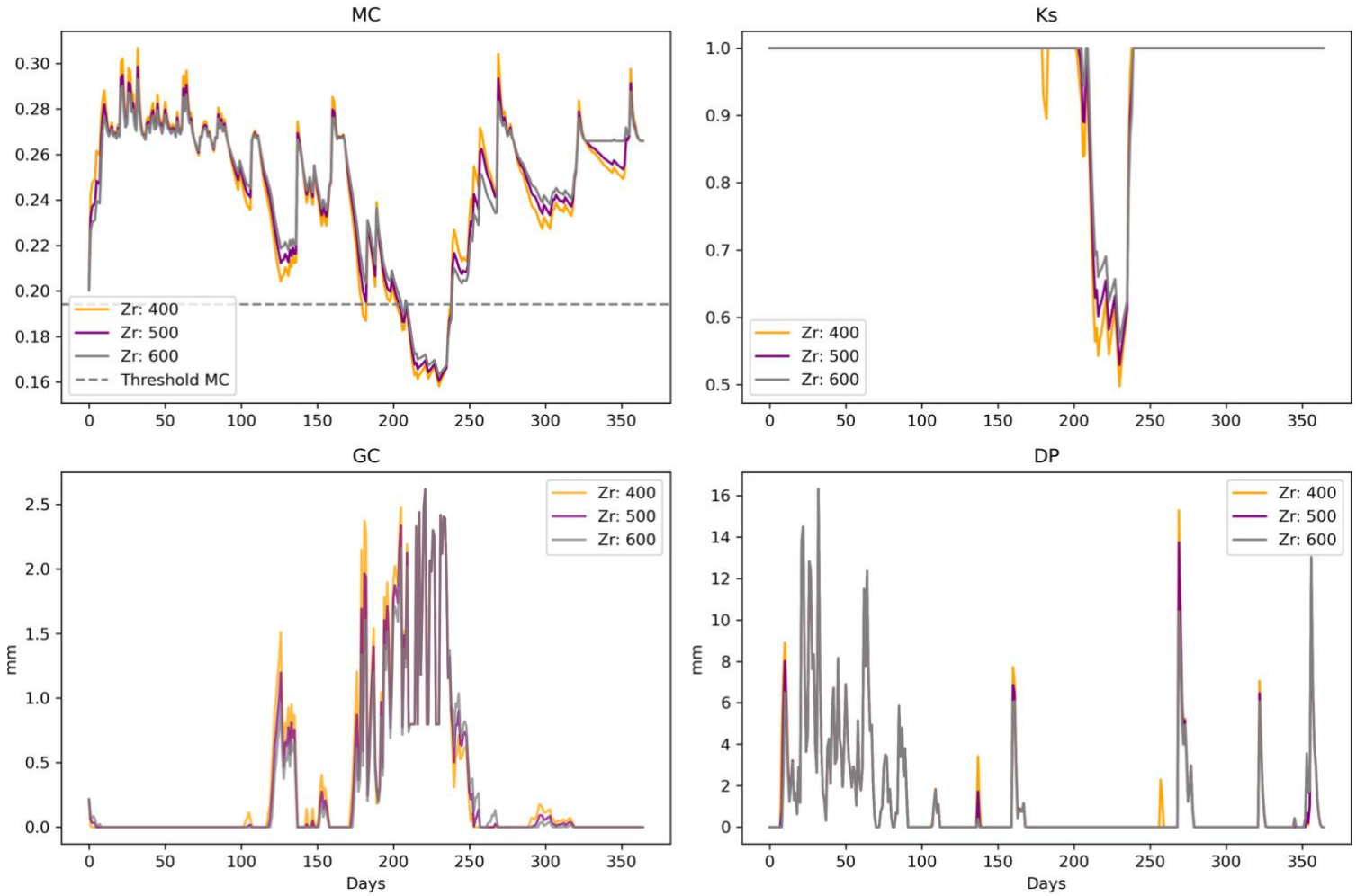

Figure 4.4: Moisture content, Ks, groundwater contribution and deep percolation for different zr values

4.2 Water storage and irrigation

When the baseline model state was proven to be working as expected, the rainwater capture, storage, and irrigation system was implemented. First, irrigation patterns are explored in section 4.2.1. Hereby, an analysis of how different vegetation types affect irrigation is done. Secondly, the flows to and from the water storage are shown in section 4.2.2. Lastly, the amount of storage capacity needed per zone to prevent water stress is presented in section 4.2.3.

4.2.1 Irrigation schedule

As mentioned in section 3.7.2, the model is set to the objective of minimizing the maximum water storage value and irrigation values in the 365-day simulation. A lower bound at the threshold moisture content is set to the moisture content to force the model to apply adequate irrigation to prevent drought stress from taking place. Figure 4.5 displays the moisture content and irrigation values for zone 1 with the reference vegetation. For the analysis of the irrigation patterns, only results from zone 1 will be presented. In the model, irrigation is a variable that is freely assigned based on how much is needed to prevent the moisture content from dropping below the threshold moisture content. Therefore, irrigation amounts are not dependent on the size of the green space as the conversion to m^3 is made in the Qti constraint.

In line with the results from section 4.1, there is a period of frequent irrigation at the time when MC is at the threshold MC. It seems that the irrigation keeps the MC at this stable level

until MC rises again and irrigation is not needed anymore. The period of irrigation starts around day 200 and irrigation values range from 1.0 to 4.0 mm. Three additional moments where irrigation takes place can be seen. At these points, there is no irrigation to be expected as the moisture content levels are not close to the threshold moisture content. Therefore, these irrigation moments do not benefit the drought resilience of the system.

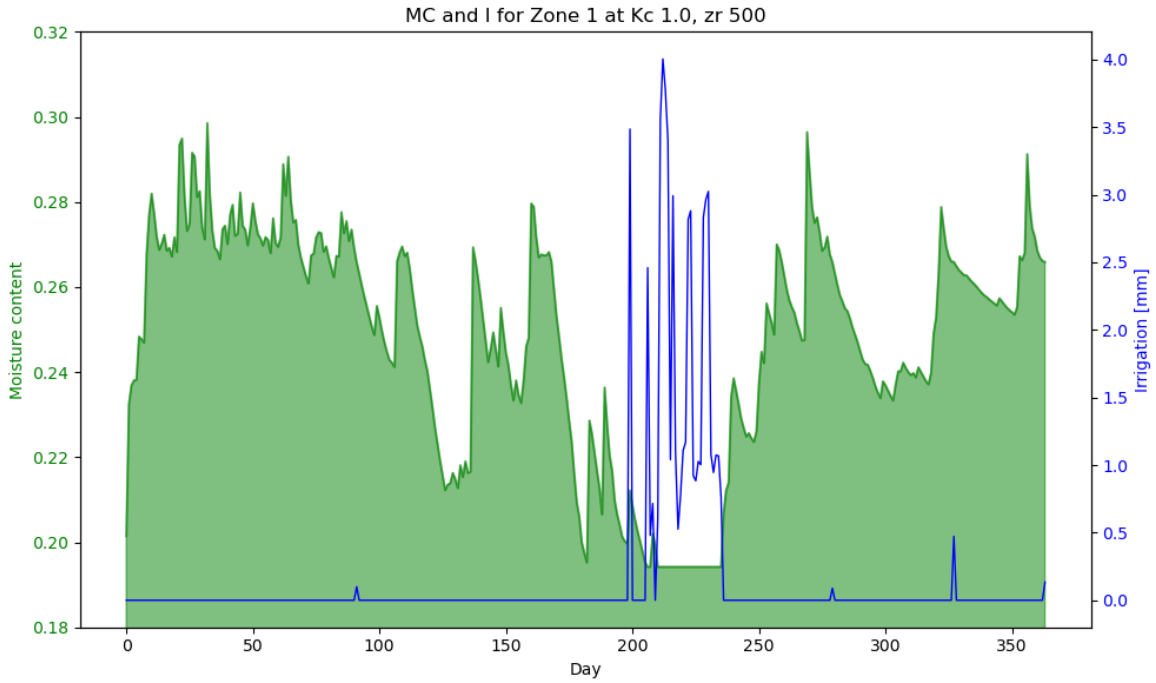

Figure 4.5: moisture content and irrigation levels for zone 1 with the reference vegetation

In Figure 4.6 the irrigation and moisture content are shown for the drought resilient vegetation. Compared to the reference vegetation irrigation, the first significant irrigation event occurs slightly later, around day 210. Additionally, less irrigation is required to keep the soil moisture content above the threshold moisture content, with exception of a large peak of 3.5 mm irrigation at the start of the summer drought period. The irrigation depth during the summer drought varies between the range of 0.5 mm and 1.0 mm. In this simulation, there are also several moments where irrigation occurs where this is not expected. Compared to figure 4.5, these moments are more frequent and longer. Near the end of the year simulation there is a period of approximately 25 days where the soil moisture content is kept at a steady value close to the field capacity. The irrigation causes the MC to stay at the field capacity value of 0.266.

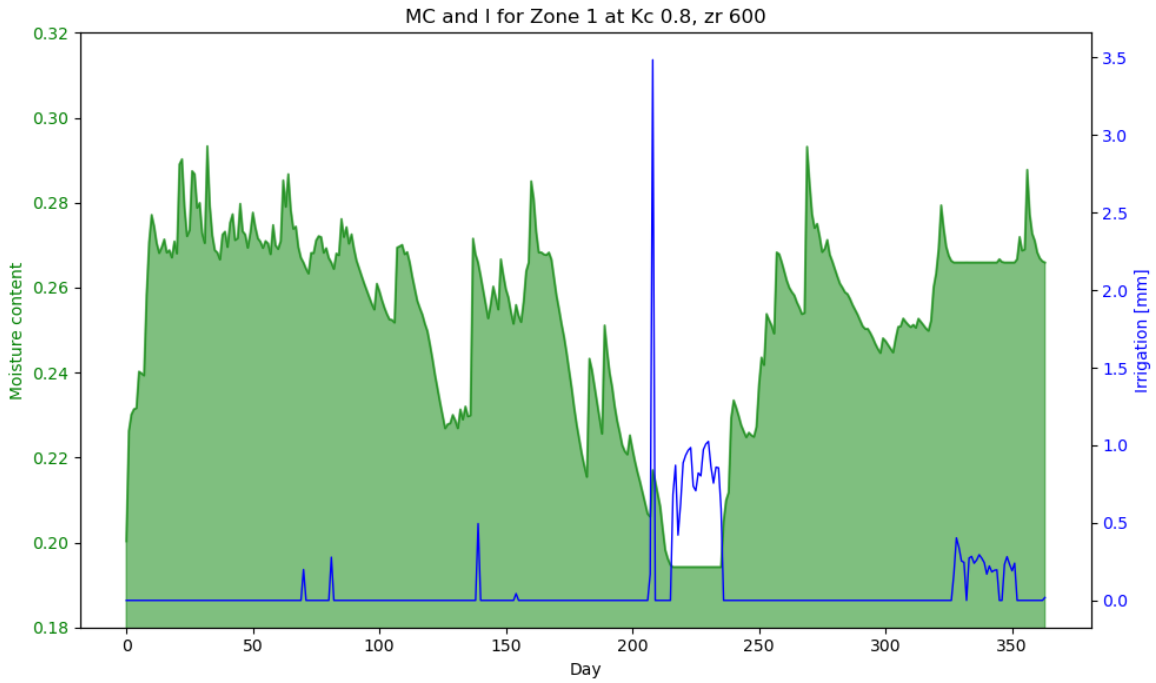

Figure 4.6: moisture content and irrigation levels for zone 1 with the drought resilient vegetation

When looking at the irrigation pattern for the drought sensitive vegetation shown in Figure 4.7, it becomes apparent that the period of frequent irrigation is longer compared to the other two scenarios. Irrigation starts earlier in the year, around day 175, and ends at the same point as in the other two scenarios. Additionally, there is a short period around day 125 when the MC is near the threshold moisture content and one irrigation event keeps the MC in the desired range. This is in line with the results seen in Figure 4.3 and 4.4 where high Kc and low zr result in a longer and more intense drought stress periods. Likewise, the amount of irrigation is nearly four times larger than the irrigation for the drought resilient vegetation. Compared to the reference vegetation, irrigation amounts are generally more similar except for one irrigation event of more than 12 mm.

At several moments, Figure 4.7 shows instances of irrigation where they are not expected. At these moments MC values are high and irrigation would not be needed.

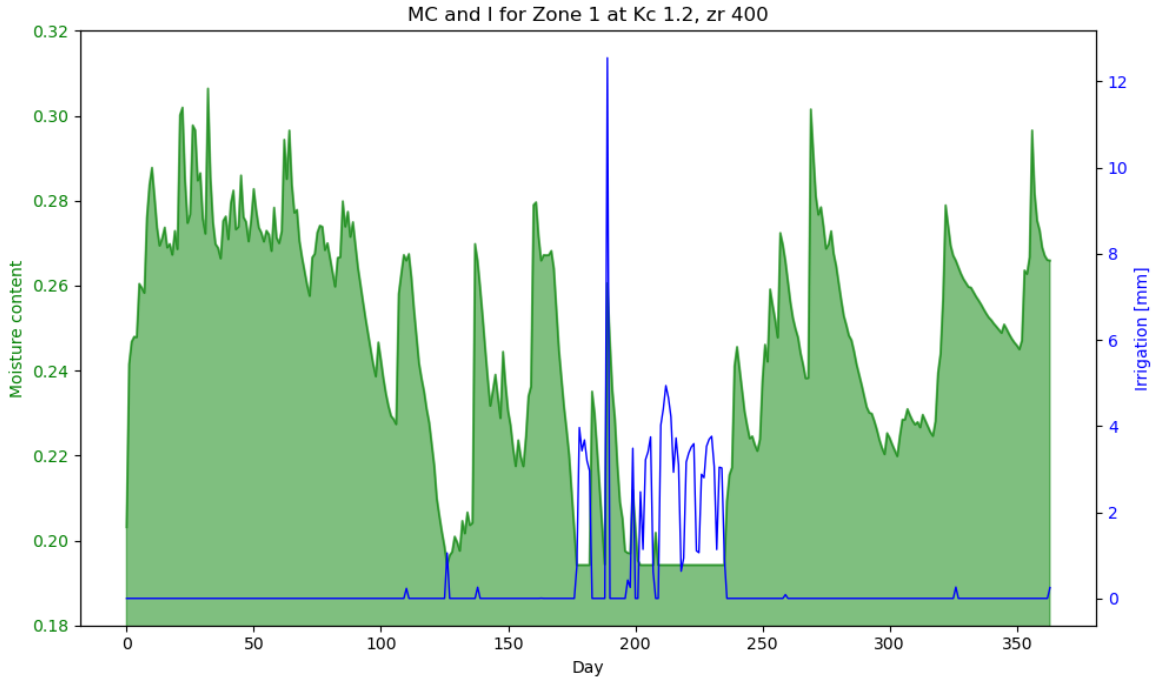

Figure 4.7: moisture content and irrigation levels for zone 1 with the drought sensitive

4.2.2 Tank flows

Resulting from the irrigation schedules, the model calculated how much water the greenspace in each zone needs. In Figure 4.8, the volume of water stored in the underground tank in zone 1 with the reference vegetation is plotted with the inflow amount from the roof and outflow to the irrigation system. Around day 155 the first water flows into the storage tank. From this point onwards there are several instances where rainwater is directed to the tank until a maximum of approximately 85 m^3 is reached at around day 200. From that point onwards, flow from the tank to the irrigation starts to occur.

When the irrigation starts, the volume in the tank is initially kept around the same amount by storing additional rainwater from the roof inflow. The water volume in the tank starts declining from approximately day 215 and eventually decreases until the tank is empty. Near the end of the year, three moments can be seen where there is a small amount of water in the tank. These moments correspond with the unexpected irrigation events seen in Figure 4.5.

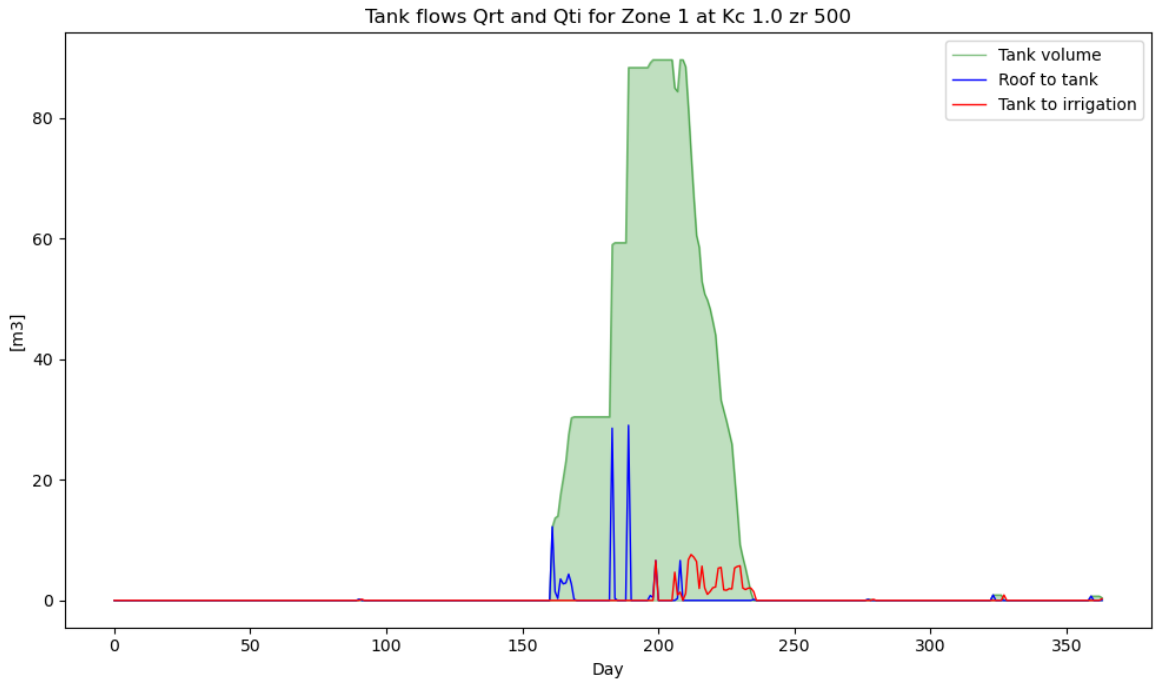

Figure 4.8: volume in the water storage tanks and the in- and outflow for the reference vegetation in zone 1

Figure 4.9 shows the water storage tank flows for the reference vegetation in zone 8. This zone is characterized by the large amount of green space in comparison to the other zones. However, compared to the result for zone 1, the same pattern in the inflow to the tank and the flow to the irrigation system can be observed. The only notable difference are the amounts, which are much higher for zone 8. Therefore, only the results from zone 1 will be shown for the drought resilient vegetation and the drought sensitive vegetation. In appendix 2, the results of zone8 for the other two vegetation types can be consulted.

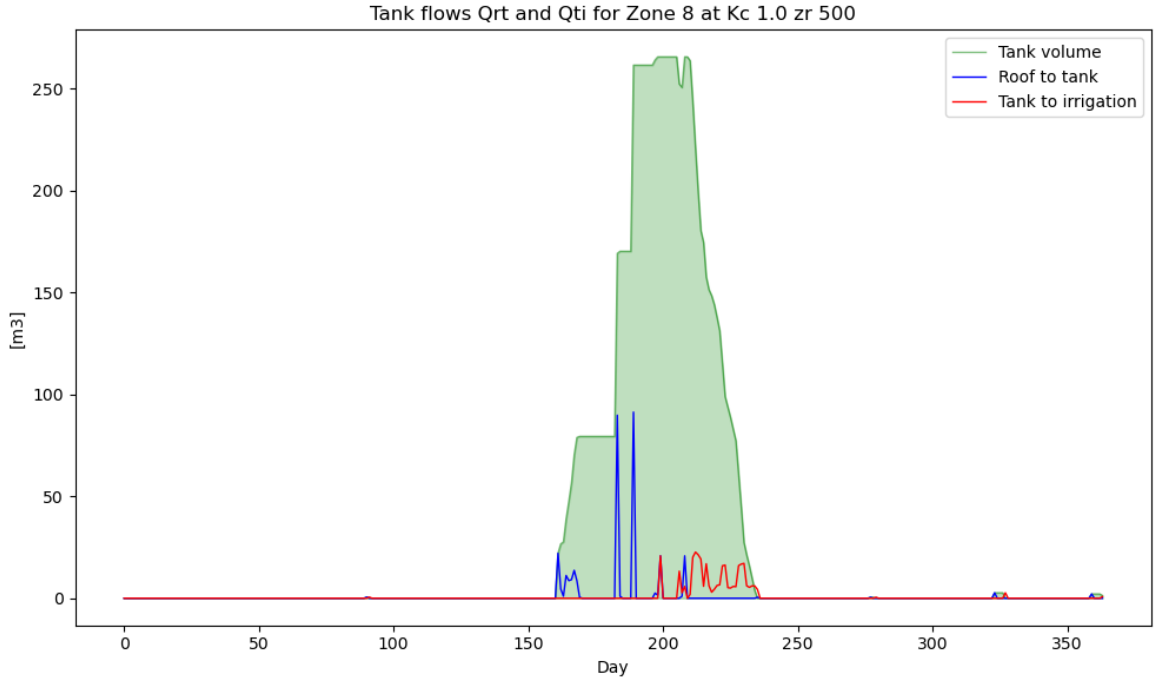

Figure 4.9: volume in the water storage tanks and the in- and outflow for the reference vegetation in zone 8

The flows to and from the tank, and the total volume in the water tank for the drought resilient vegetation are shown in Figure 4.10. Compared to the reference vegetation results in Figure 4.8, the inflow to the storage tank for the drought resilient vegetation starts at a later point in the year. In two moments, the storage amount is filled to approximately 31 m^3. Following the irrigation pattern seen in Figure 4.6, the flow from the tank to the irrigation system starts several days later compared to the reference vegetation irrigation pattern. Additionally, the irrigation period at the end of the year which is visible in Figure 4.6 results in a short period of inflow to the water tank. Hereafter, the flow to the irrigation system slowly drains the storage tank.

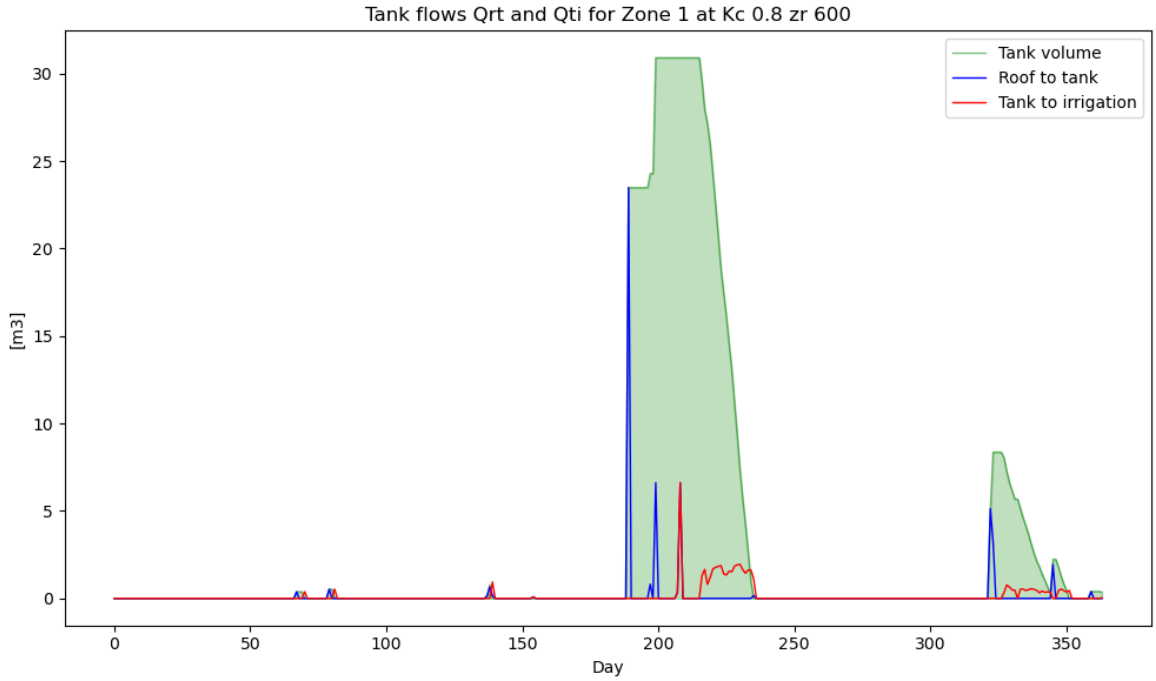

Figure 4.10: volume in the water storage tanks and the in- and outflow for the drought resilient vegetation in zone 1

Figure 4.11 shows the water storage tank flows for the drought sensitive vegetation. The first significant moment where water flows to the storage tank is around day 140. During a period of approximately 30 days, the storage amount gradually increases to approximately 160 m^3 of water. Water flow to the irrigation system starts occurring from around day 175.

The difference between the vegetation types is the amount of water that is stored in the tank. Expected due to the difference in irrigation depth. Also, for the more drought sensitive vegetation, the inflow to the water tank starts earlier in the spring months. Almost 100 days compared to the drought resilient vegetation. Overall, the tanks are empty again when the summer drought ends, at the same moment as for the other two vegetation types.

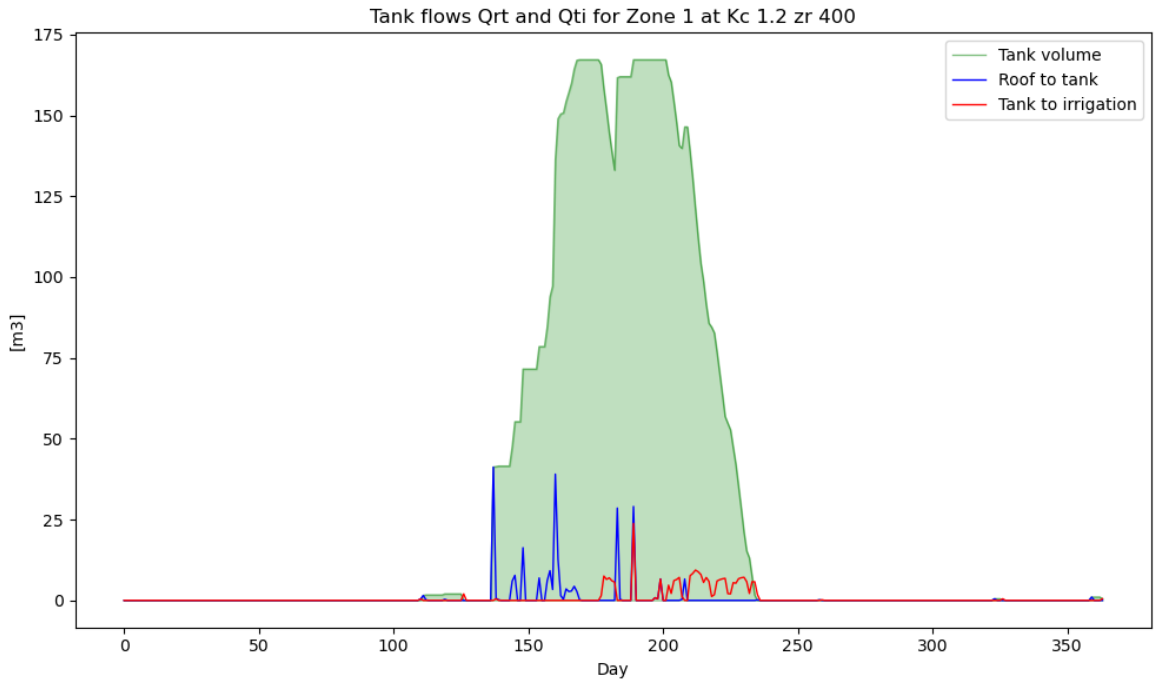

Figure 4.11: volume in the water storage tanks and the in- and outflow for the drought sensitive vegetation in zone 1

4.2.3 Storage amount

Results for the maximum storage capacity that was reached per zone in the simulations for the three vegetation types are shown in Figure 4.12. It immediately becomes apparent that zone 8 has 3 times more storage capacity demand than the other zones. Additionally, there is a large difference in the irrigation water needs between the vegetation types. Generally, the larger the total amount of water needed, the larger the difference between the vegetation types becomes.

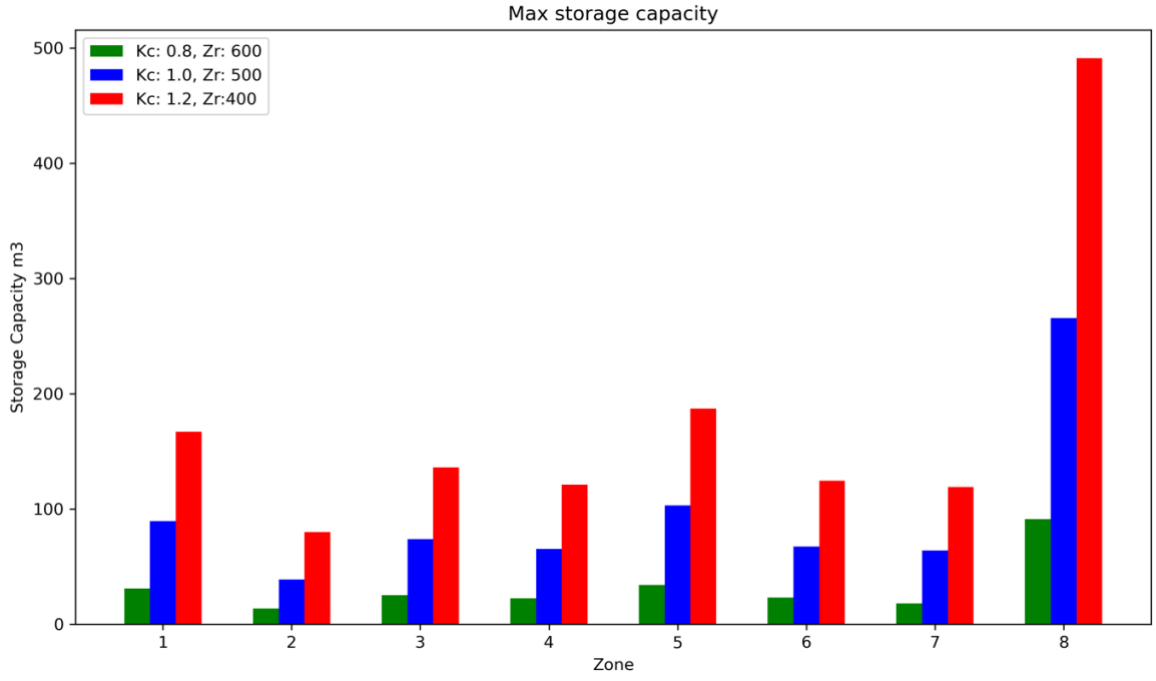

Figure 4.12: maximum storage capacity reached per zone and vegetation

However, not much can be said about this figure without comparing the data with the maximum storage space which is available per zone. Figure 4.13 shows what percentage of the total size of the underground storage tanks must be used to maintain the drought summer without water stress. Unlike the impression given in Figure 4.12, zones 1 and 2 have the highest percentages of required water storage. A large difference can be seen between the different vegetation types, where the drought sensitive vegetation requires almost double the amount of storage compared to the reference vegetation. For zone one, the drought sensitive vegetation requires more than one-third of the storage tank size for irrigation water. When comparing the drought resilient vegetation and the drought sensitive vegetation, the required water storage for the drought sensitive vegetation is more than five times greater.

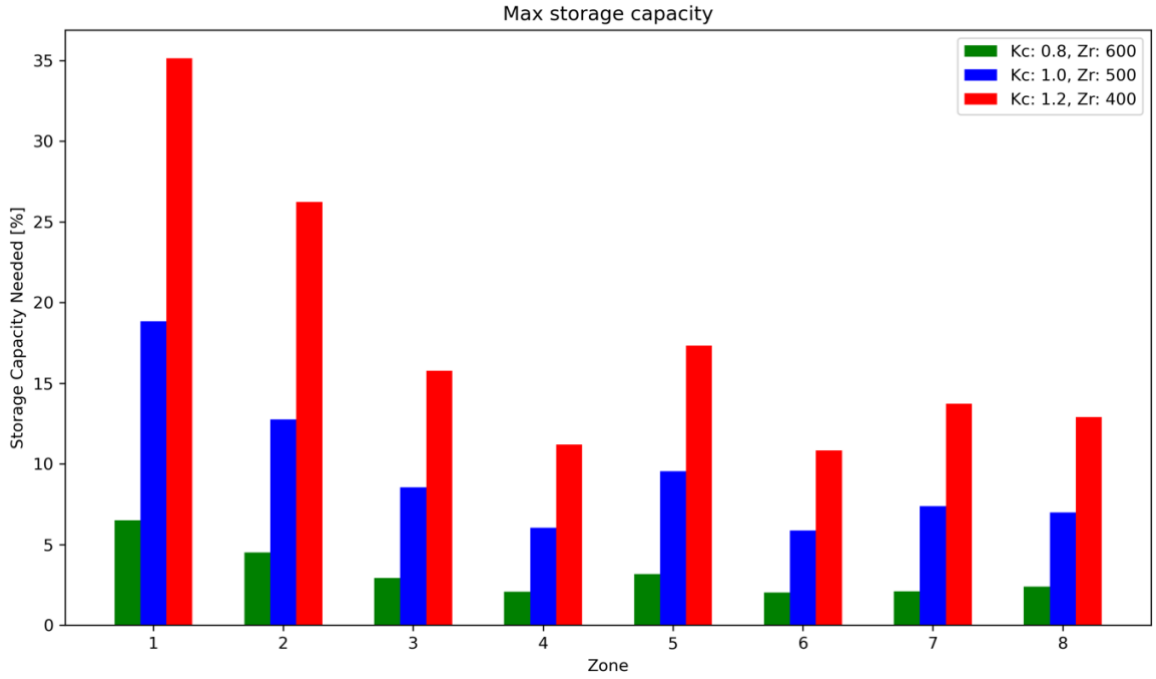

Figure 4.13: percentage of storage capacity use per zone and vegetation

These results are from a simulation where there is no exchange of stored irrigation water between zones. When unlimited water exchange between zones is possible, the storage capacity can be treated for a single zone. The storage capacity needed for irrigation of reference vegetation is 7.97%, for the drought resilient vegetation 2.69%, and for the drought sensitive vegetation 14.80%.

5. Discussion

In this chapter, the results of the scenario analysis for the Bajeskwartier drought resilience model are discussed. First, a reflection on the baseline non-irrigation model performance is presented. Second, the effect of vegetation properties on the water system of the Bajeskwartier is outlined. Third, the rainwater capture, storage, and irrigation system dynamics are discussed. Lastly, a reflection on the limitations of the model is made.

5.1 Baseline model performance

In the non-irrigation state, the model appears to be functioning as intended. Soil processes exhibit the expected behavior, with MC levels following a seasonal pattern. During the winter months, MC starts at higher levels, gradually decreasing throughout the spring and summer, and experiencing a subsequent rise in autumn. Groundwater contribution becomes prominent when MC reaches lower values, while deep percolation (DP) occurs during periods of high MC coupled with significant precipitation events. This verification of the expected soil moisture dynamics is a positive indicator of the capacity of the model to simulate the fundamental soil water balance processes.

Evapotranspiration is an important aspect of the soil moisture balance, as represents the water use of the vegetation. Therefore, it is important that the modeled ETa closely resembles patterns observed in the real world. As shown in Figure 4.2, ETa and ET_0 follow an expected seasonal trend where values are generally low in the colder months, and high in the warmer summer months. However, ET0 rates seem to be slightly on the low side. In the summer months, the ET0 values range between approximately 3 and 4 mm/day. For the Dutch climate, the FAO describes ET0 rates to be between 3 to 4 mm/day for temperatures between 15 and 25°C (Brouwer et al., 1989). However, when comparing the period where the highest ET0 takes place with the input temperature data, the daily average temperatures are often significantly higher than the 15 to 25°C range (appendix 1). Higher temperatures are associated with ET0 values in the range of 5-6 mm/day. This behavior might result in an underestimation of the drought stress. Therefore, it is important to take this into account.

5.2 Vegetation properties

In this section, we delve into the impact of two crucial parameters, zr and Kc, on the soil moisture balance within our model. These factors play an important role in shaping the resilience and stability of the system to weather conditions and drought events. In the analysis of vegetation characteristics, Kc has a large effect on the MC through the ETa. This shows in the results that at first sight, Kc has a greater influence on the MC than the zr. However, one notable finding is that deeper rooting depths tend to result in less extreme peaks in the soil moisture balance. This observation suggests that systems with deeper root zones have greater stability and resilience to fluctuations in weather patterns. Deeper roots offer an extended reach into the soil profile, enabling the vegetation to access moisture stored deeper in the ground, thus mitigating the impact of surface-level moisture fluctuations. Furthermore, DP for the zr parameter only differs after a prolonged period without DP. This pattern may be attributed to the quicker rate at which soil moisture reaches the field capacity in systems with a deeper zr.

When assessing the length of the drought stress periods for the different vegetation properties, the question of how much drought stress is tolerable for the vegetation arises. It might be the case that specific vegetation can endure short periods of drought stress without suffering permanent damage. If this is the case, then a very drought-resistant set of vegetation might be sufficient to remain healthy without any irrigation. It is important to note that the vegetation types in this model are not a real-world representation but a means to assess how vegetation influences drought resilience.

5.3 Irrigation model state

The implementation of the rainwater capture, storage, and irrigation system has been shown to result in a well-functioning system that can prevent drought stress in the Bajeskwartier. When assessing the irrigation depths for the three vegetation scenarios, they are well below the upper bound set in the problem formulation. For every scenario, the irrigation depths are within a reasonable range when compared to FAO irrigation scheduling guidelines (Brouwer et al., 1989). This reaffirms the effectiveness of the modeling method in calculating irrigation demand for different vegetation types. However, it is important to note that the irrigation results show occasional irregularities in the form of minor irrigation events when the MC is well above the threshold moisture content. These peaks are likely computational artifacts and do not appear to significantly impact the overall model performance. Nonetheless, it is worth noting that computational limits were encountered when attempting to set a constraint to prevent irrigation from taking place when MC is higher than the field capacity. Addressing this model limitation should be considered in future research.

The water flows to and from the underground storage tanks show a pattern where the tanks are filled well before the first irrigation starts. Depending on the vegetation type, inflow to the storage tank starts in the early or late months of spring. Most water that is stored is gathered in that period, except for occasional water inflow in the summer. This is due to the high amount of precipitation in the spring months and the dry summer months. While this water storage pattern is optimized for this current climate scenario, an important takeaway is that inflow to the storage tank should take place well before the expected driest months.

Regarding rainwater storage size, the results show that, for all vegetation types in all zones, there is sufficient storage capacity to meet the water demand of a 1-in-30-year drought event in a climate change scenario for 2085. The minimum percentage of the tank that should be allocated to water storage varies greatly. For zones one and two, these percentages are much higher than for the other zones. However, when the storage and irrigation systems of the different zones can be connected, a more even distribution of water storage can take place. In this system state, it is advisable to allocate between 2.69% and 14.80% of the storage capacity for rainwater storage. This amount should be present in the tank from the spring onwards and maintained as close to the desired amount as possible. Even for the scenario with the drought sensitive vegetation, it is a relatively small percentage of the tank volume to allocate for irrigation water storage. In instances of intense rainfall events when water buffering is required, the tanks can be temporarily filled to the maximum volume, whereafter the excess water can be slowly drained to the desired volume. Notably, rainwater storage is primarily necessary for the spring and summer, so in the winter, when most precipitation is, the full potential buffer capacity can be utilized.

While this research focuses on the Bajeskwartier case, the adaptability of the method to other cases has been considered. All input data regarding the climate scenario, green space, water storage, and water catchment sizes can be changed according to the new situation. Likewise, the vegetation and soil specifications can be altered. This method provides a valuable starting point for assessing drought sensitivity in different contexts.

5.4 Research limitations

While exploring the Bajeskwartier drought resilience model, several limitations should be acknowledged. First, the simulations conducted in this research are based on a static year of climate data where the climate conditions throughout the year are predetermined. Weather patterns are unpredictable except for a few days in advance. Therefore, the development of an additional dynamic water management strategy is needed to adapt to real-time climate variability. Nevertheless, this research provides valuable insights into the water demand and

how much potential water storage demand, which can be a foundation for a dynamic water management method.

Secondly, the model does not consider the evaporation of irrigation water. Currently, the model assumes that all irrigation water reaches the soil. Depending on the irrigation system, a part of the irrigated water might not enter the soil due to losses from evaporation and other factors (Urrego-Pereira et al., 2013). Therefore, the actual irrigation demand might be higher than what the results of this research show. Additionally, the irrigation depths in the model represent the minimum required to prevent drought stress. It will be difficult to precisely monitor the soil to keep the MC at this exact amount when the exact amount of water that reaches the soil is uncertain.

Thirdly, in the assessment of the rainwater storage allocation, no assessment has been made of the sufficiency of the buffer capacity when the tank is filled with water for irrigation. While the percentage of the water storage tank that should be allocated to irrigation water storage is seemingly low, it might occur that there are intense rainfall events where the total buffer capacity would be needed. The inclusion of a rainwater drainage system in the model would provide insights into whether the storage tank can adequately accommodate maximum irrigation volume requirements without exceeding the limits.

Fourth, the current time resolution is daily. Total daily precipitation amounts are combined with daily mean values for temperature, solar radiation, among others. In averaging the daily weather patterns, extreme values can be canceled out which might underestimate the severity of weather extremes. Therefore, it is advisable that the possibilities of increasing the model resolution to hourly data are explored in future research.

Lastly, there are several limitations due to the input data used in the model. As mentioned, the vegetation types considered in this study represent hypothetical vegetation to assess the behavior of the model. These do not correspond to real-world vegetation types and the model could become more accurate when more consideration is taken in the use of vegetation types. Additionally, the current model is based on a single climate scenario. As climate change scenarios are essential in understanding future weather patterns, more comprehensive testing of how the model responds to different climate change projections is needed. Exploring the model behavior under various climate change scenarios will gain insights into the patterns of inflow to the storage tanks in a different simulation year. Using this knowledge, better estimations can be made as to when the storage tank should be filled with water for irrigation.

6. Conclusion

This research aimed to create a digital representation of the Bajeskwartier water system to assess what modeling approach could quantify the Bajeskwartier drought resilience under a future climate change scenario. While vegetation water demand models generally address agricultural systems, the approach in this research provides a method that is tailor-made to urban environments. A digital representation of the Bajeskwartier water system was developed to model the soil moisture balance in combination with a rainwater capture, storage, and irrigation optimization system. By combining local soil and vegetation characteristics and KNMI climate scenarios, analyses have been made of the dynamics between the soil processes and climate conditions. Key processes that regulate the water flows into, through, and out of the soil were shown to be implemented in an accurate way in this first version of the model.

By incorporating a scenario planning approach, the behavior of the model was tested according to various vegetation types. The analysis of the effects of the zr and Kc on the soil moisture balance has revealed the relationships between these parameters and their role in influencing system resilience. Deeper rooting depths provide stability against irregular weather patterns, while Kc directly influences vegetation water demand, making it a key determinant of soil moisture dynamics.

Additionally, the irrigation system optimization proved to be effective in mitigation of drought stress. When combined with the rainwater capture and storage system, the optimal water resource allocation approach resulted in clear insights into the water requirements to mitigate drought stress. The results show that there is sufficient water storage capacity to meet the demand for a 1-in-30-year drought for a 2085 climate scenario. Nevertheless, careful coordination of water capture, storage, and irrigation is required to maximize the effectiveness of the system. Notably, the Bajeskwartier possesses sufficient water storage possibility to mitigate drought stress even for drought sensitive vegetation.

6.1 Further research

While this research provides a promising methodology for urban drought management practices, future research can further improve the model performance and address the current limitations. An additional analysis and verification of the evapotranspiration part of the model is advisable, especially in combination with an in-depth investigation of site-specific vegetation types. This way, the accuracy of the vegetation water demand can be further improved. Additionally, testing the model with additional climate scenarios is advised.

8. References

Ailliot, P., Allard, D., Monbet, V., & Naveau, P. (2015). *Stochastic weather generators: an overview of weather type models*.

Allen, R. G., Pereira, L. S., Raes, D., & Smith, M. (1998). *Crop evapotranspiration - Guidelines for computing crop water requirements - FAO Irrigation and drainage paper 56*. Food and Agricultural Organisation of the United Nations. https://www.researchgate.net/publication/235704197

AM, & Fabrications. (2020). *Voortgangsrapportage Voorlopig Ontwerp*.

Angou, G., IJzermans, E., Joosse, N. F. E., van Muilekom, L. V., & van der Plas, J. W. (2022). *Water Shortage Model*.

Arnold, R. D., & Wade, J. P. (2015). A definition of systems thinking: A systems approach. *Procedia Computer Science*, *44*(C), 669–678. https://doi.org/10.1016/j.procs.2015.03.050

Balogun, A. L., Marks, D., Sharma, R., Shekhar, H., Balmes, C., Maheng, D., Arshad, A., & Salehi, P. (2020). Assessing the Potentials of Digitalization as a Tool for Climate Change Adaptation and Sustainable Development in Urban Centres. *Sustainable Cities and Society*, *53*. https://doi.org/10.1016/j.scs.2019.101888

Bréda, N. J. J. (2003). Ground-based measurements of leaf area index: A review of methods, instruments and current controversies. In *Journal of Experimental Botany* (Vol. 54, Issue 392, pp. 2403–2417). https://doi.org/10.1093/jxb/erg263

Brouwer, C., Prins, K., Kay, M., & Heibloem, M. (1989). *Irrigation Water Management: Irrigation Methods*. FAO - Food and Agriculture Organization of the United Nations.

Castellaro, G., Morales, L., Ahumada, M., & Barozzi, A. (2010). Simulation of dry matter productivity and water dynamics in a Chilean Patagonian range. *Chilean Journal of Agricultural Research*, *70*(3), 417–427.

Chen, J., & Brissette, F. P. (2014). Comparison of five stochastic weather generators in simulating daily precipitation and temperature for the Loess Plateau of China. *International Journal of Climatology*, *34*(10), 3089–3105. https://doi.org/10.1002/joc.3896

Chen, Q., Johnson, E. S., Bernal, D. E., Valentin, R., Kale, S., Bates, J., Siirola, J. D., & Grossmann, I. E. (2022). Pyomo.GDP: an ecosystem for logic based modeling and optimization development. *Optimization and Engineering*, *23*(1), 607–642. https://doi.org/10.1007/s11081-021-09601-7

D'Ambrosio, C., Lodi, A., Wiese, S., & Bragalli, C. (2015). Mathematical programming techniques in water network optimization. *European Journal of Operational Research*, *243*(3), 774–788. https://doi.org/10.1016/j.ejor.2014.12.039

Duarte Rocha, A., Vulova, S., van der Tol, C., Förster, M., & Kleinschmit, B. (2022). Modelling hourly evapotranspiration in urban environments with SCOPE using open remote sensing and meteorological data. *Hydrology and Earth System Sciences*, *26*(4), 1111–1129. https://doi.org/10.5194/hess-26-1111-2022

Fan, Y., Miguez-Macho, G., Jobbágy, E. G., Jackson, R. B., & Otero-Casal, C. (2017). Hydrologic regulation of plant rooting depth. *Proceedings of the National Academy of Sciences of the United States of America*, *114*(40), 10572–10577. https://doi.org/10.1073/pnas.1712381114

Fooladivanda, D., & Taylor, J. A. (2015, December 18). Optimal Pump Scheduling and Water Flow in Water Distribution Networks. *2015 IEEE 54th Annual Conference on Decision and Control (CDC)*.

Foster, J., Lowe, A., & Winkelman, S. (2011). *The Value of Green Infrastructure for Urban Climate Adaptation*. www.ccap.org.

Gao, X., Huo, Z., Qu, Z., Xu, X., Huang, G., & Steenhuis, T. S. (2017). Modeling contribution of shallow groundwater to evapotranspiration and yield of maize in an arid area. *Scientific Reports*, *7*, 1–13. https://doi.org/10.1038/srep43122

IPCC. (2013). Summary for Policymakers. In T. F. Stocker, D. Qin, G.-K. Plattner, M. Tignor, S. K. Allen, J. Boschung, A. Nauels, Y. Xia, V. Bex, & P. M. Midgley (Eds.), *Climate Change 2013: The Physical Science Basis. Contribution of Working Group I to the Fifth Assessment Report of the Intergovernmental Panel on Climate Change*. Cambridge University Press.

KNMI. (2021). *KNMI Klimaatsignaal '21: Hoe het klimaat in Nederland snel verandert*.

KNMI. (2022, October 3). *Niet eerder deze eeuw zo droog als dit jaar*. https://www.knmi.nl/over-het-knmi/nieuws/droge-zomerhalfjaar-van-2022

Lawrence, D. J., Runyon, A. N., Gross, J. E., Schuurman, G. W., & Miller, B. W. (2021). Divergent, plausible, and relevant climate futures for near- and long-term resource planning. *Climatic Change*, *167*(3–4). https://doi.org/10.1007/s10584-021-03169-y

Lee, S., & Grossmann, I. E. (2001). *A Global Optimization Algorithm for Nonconvex Generalized Disjunctive Programming and Applications to Process Systems*. https://doi.org/10.1016/S0098-1354(01)00732-3

Liu, D., Guo, S., Shao, Q., Liu, P., Xiong, L., Wang, L., Hong, X., Xu, Y., & Wang, Z. (2018). Assessing the effects of adaptation measures on optimal water resources allocation under varied water availability conditions. *Journal of Hydrology*, *556*, 759–774. https://doi.org/10.1016/j.jhydrol.2017.12.002

Liu, Y., Pereira, L. S., & Fernando, R. M. (2006). Fluxes through the bottom boundary of the root zone in silty soils: Parametric approaches to estimate groundwater contribution and percolation. *Agricultural Water Management*, *84*(1–2), 27–40. https://doi.org/10.1016/j.agwat.2006.01.018

Monat, J. P., & Gannon, T. F. (2015). What is Systems Thinking? A Review of Selected Literature Plus Recommendations. *American Journal of Systems Science*, *2015*(1), 11–26. https://doi.org/10.5923/j.ajss.20150401.02

Pereira, L. S., & Alves, I. (2005). *Crop Water Requirements*.

Rai, R. K., Singh, V. P., & Upadhyay, A. (2017). Soil Analysis. In *Planning and Evaluation of Irrigation Projects* (pp. 505–523). Elsevier. https://doi.org/10.1016/B978-0-12-811748-4.00017-0

Scurlock, J. M. 0, Asner, G. P., & Gower, S. T. (2001). *Worldwide Historical Estimates of Leaf Area Index, 1932-2000 ORNL-27 (4-00)*. http://www.osti.gov/contact.htmI

Seneviratne, S. I., Zhang, X., Adnan, M., Badi, W., Dereczynski, C., Di Luca, A., Ghosh, S., Iskandar, I., Kossin, J., Lewis, S., Otto, F., Pinto, I., Satoh, M., Vicente-Serrano, S. M., Wehner, M., & Zhou, B. (2021). Weather and Climate Extreme Events in a Changing Climate. In V. Masson-Delmotte, P. Zhai, A. Pirani, S. L. Connors, C. Péan, S. Berger, N. Caud, Y. Chen, L. Goldfarb, M. I. Gomis, M. Huang, K. Leitzell, E. Lonnoy, J. B. R. Matthews, T. K. Maycock, T. Waterfield, O. Yelekçi, R. Yu, & B. Zhou (Eds.), *Climate Change 2021: The Physical Science Basis. Contribution of Working Grou p I to the Sixth Assessment Report of the Intergovernmental Panel on Climate C hange* (Vol. 6, Issue Spain). Cambridge University Press. https://doi.org/10.1017/9781009157896.013

Star, J., Rowland, E. L., Black, M. E., Enquist, C. A. F., Garfin, G., Hoffman, C. H., Hartmann, H., Jacobs, K. L., Moss, R. H., & Waple, A. M. (2016). Supporting adaptation decisions through scenario planning: Enabling the effective use of multiple methods. *Climate Risk Management*, *13*, 88–94. https://doi.org/10.1016/j.crm.2016.08.001

Sweco. (2020). *Notitie Waterparagraaf Bajes Kwartier*.

Urrego-Pereira, Y. F., Martínez-Cob, A., & Cavero, J. (2013). Relevance of Sprinkler Irrigation Time and Water Losses on Maize Yield. *Agronomy Journal*, *105*(3), 845–853. https://doi.org/10.2134/agronj2012.0488

Van Den Hurk, B., Siegmund, P., & Klein Tank, A. (2014). *KNMI'14: Climate Change scenarios for the 21st Century-A Netherlands perspective*. www.climatescenarios.nl

Van Genuchten, M. T., Leij, F. J., & Yates, S. R. (1991). *The RETC Code for Quantifying the Hydraulic Functions of Unsaturated Soils*.

Ward, S., Memon, F. A., & Butler, D. (2012). Performance of a large building rainwater harvesting system. *Water Research*, *46*(16), 5127–5134. https://doi.org/10.1016/j.watres.2012.06.043

Zeleke, K. T., & Wade, L. J. (2012). Evapotranspiration Estimation Using Soil Water Balance, Weather and Crop Data. In *Evapotranspiration-Remote sensing and modeling* (pp. 41–58). www.intechopen.com

9. Appendix

9.1 Appendix 1

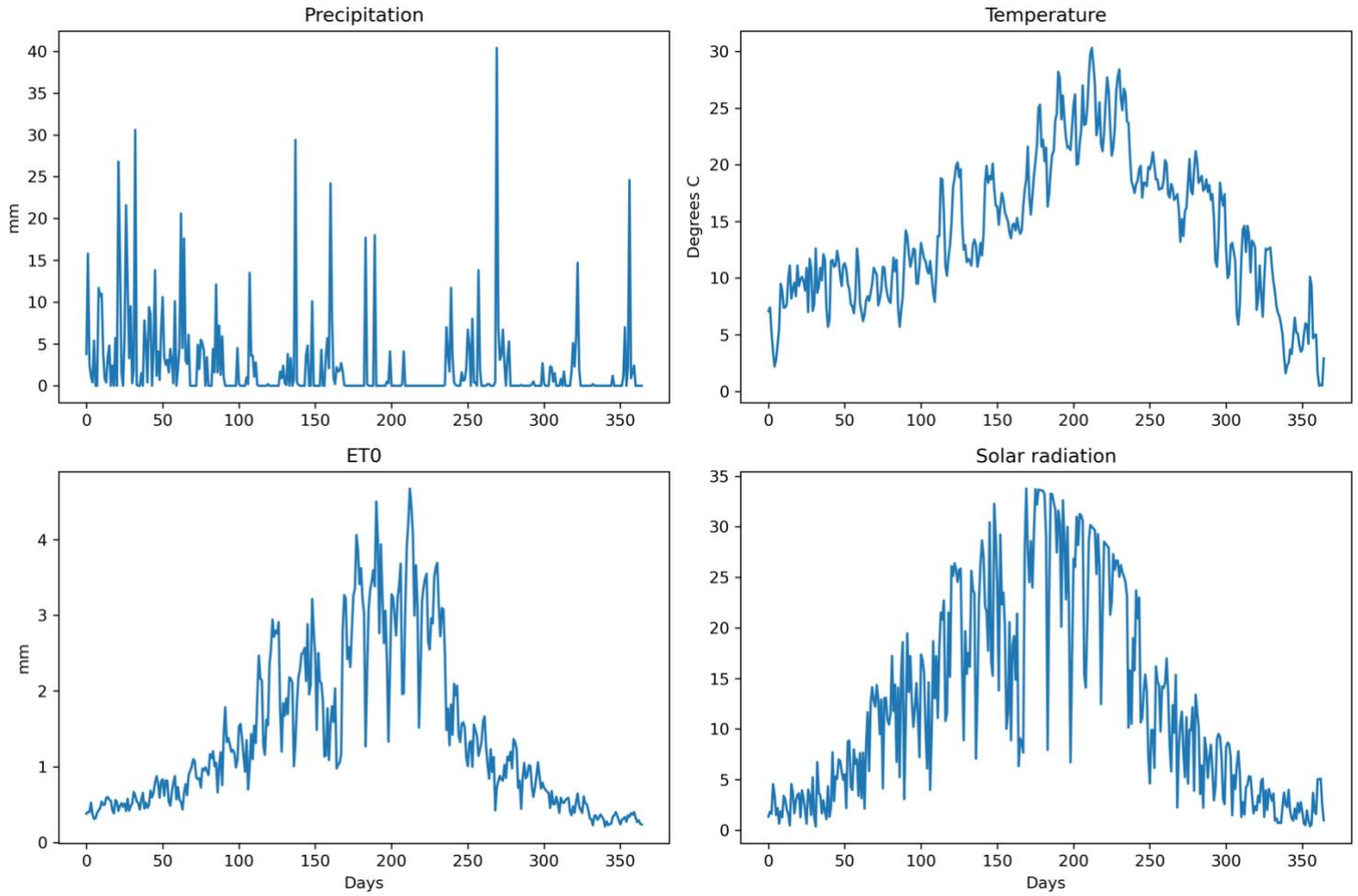

Precipitation, temperature, ET0, and solar radiation data generated in the preprocessing stage. This data is input for the optimization problem.

9.2 Appendix 2

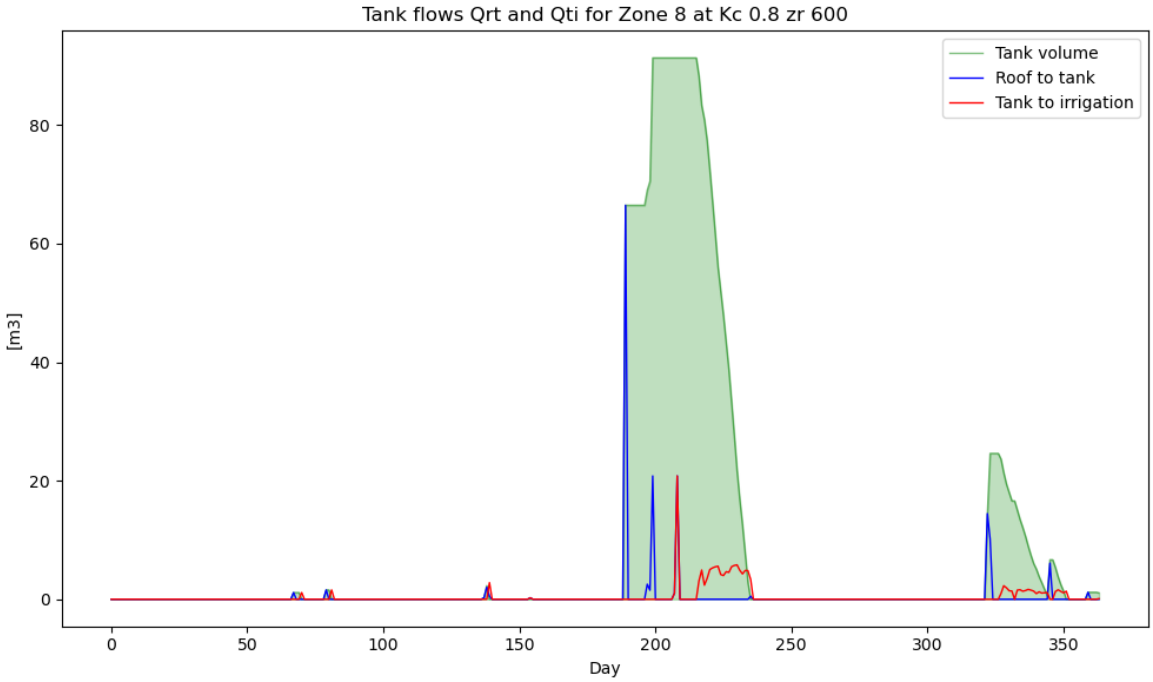

Volume in the water storage tanks and the in- and outflow for the drought resilient vegetation in zone 8

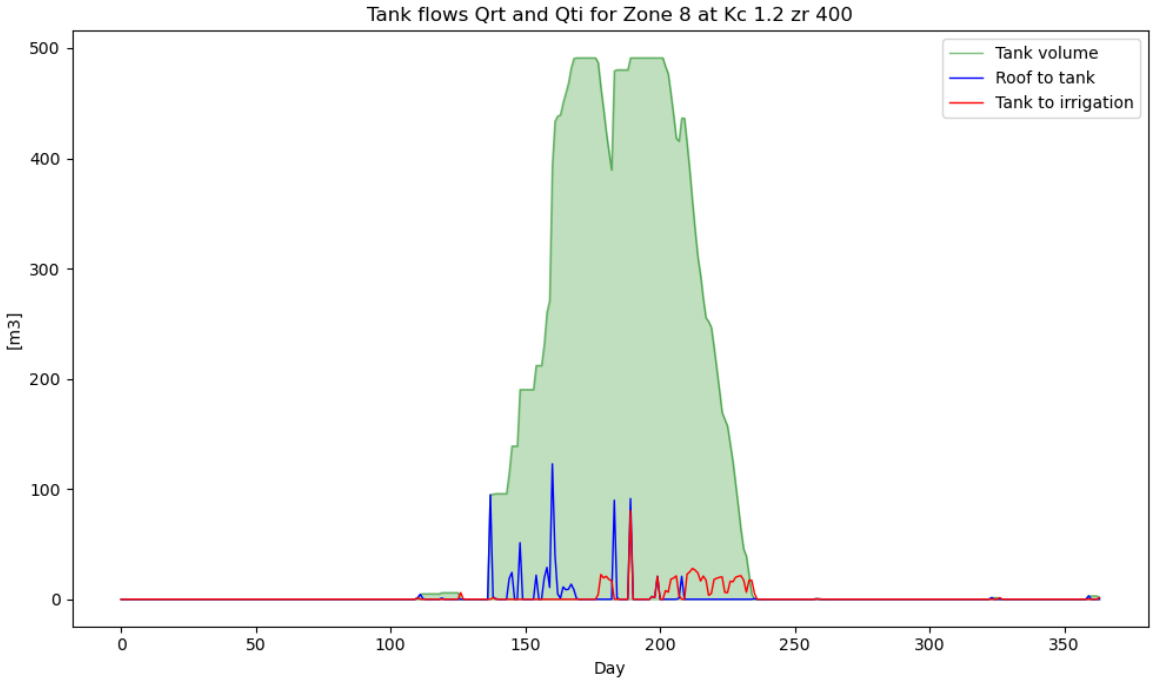

Volume in the water storage tanks and the in- and outflow for the drought sensitive vegetation in zone 8